BARC/2009/E/007

NDDP MULTI-STAGE FLASH DESALINATION PROCESS SIMULATOR DESIGN "PROCESS OPTIMIZATION"

by

G.N. Sashi Kumar, A.K. Mahendra, A. Sanyal and G. Gouthaman
Machine Dynamics Division
Chemical Technology Group

2009

BARC/2009/E/007

BARC/2009/E/007

GOVERNMENT OF INDIA
ATOMIC ENERGY COMMISSION

NDDP MULTI-STAGE FLASH DESALINATION PROCESS SIMULATOR DESIGN "PROCESS OPTIMIZATION"

by

G.N. Sashi Kumar, A.K. Mahendra, A. Sanyal and G. Gouthaman
Machine Dynamics Division
Chemical Technology Group

BHABHA ATOMIC RESEARCH CENTRE
MUMBAI, INDIA
2009

BIBLIOGRAPHIC DESCRIPTION SHEET FOR TECHNICAL REPORT
(as per IS : 9400 - 1980)

01	*Security classification :*	Unclassified
02	*Distribution :*	External
03	*Report status :*	New
04	*Series :*	BARC External
05	*Report type :*	Technical Report
06	*Report No. :*	BARC/2009/E/007
07	*Part No. or Volume No. :*	
08	*Contract No. :*	
10	*Title and subtitle :*	NDDP multi-stage flash desalination process simulator design 'Process Optimization'
11	*Collation :*	53 p., figs., 2 tabs., 2 ills.
13	*Project No. :*	
20	*Personal author(s) :*	G.N. Sashi Kumar; A.K. Mahendra; A. Sanyal; G. Gouthaman
21	*Affiliation of author(s) :*	Machine Dynamics Division, Bhabha Atomic Research Centre, Mumbai
22	Corporate author(s) :	Bhabha Atomic Research Centre, Mumbai-400 085
23	*Originating unit :*	Machine Dynamics Division, Chemical Technology Group, BARC, Mumbai
24	*Sponsor(s) Name :*	Department of Atomic Energy
	Type :	Government

Contd...

30	*Date of submission :*	February 2009
31	*Publication/Issue date :*	March 2009
40	*Publisher/Distributor :*	Associate Director, Knowledge Management Group and Head, Scientific Information Resource Division, Bhabha Atomic Research Centre, Mumbai
42	*Form of distribution :*	Hard copy
50	*Language of text :*	English
51	*Language of summary :*	English, Hindi
52	*No. of references :*	26 refs.
53	*Gives data on :*	

60 *Abstract :* The improvement of NDDP-MSF plant's performance ratio (PR) from design value of 9.0 to 13.1 was achieved by optimizing the plant's operating parameters within the feasible zone of operation. This plant has 20% excess heat transfer area over the design condition which helped us to get a PR of 15.1 after optimization. Thus we have obtained, (1) A 45% increase in the output over design value by the optimization carried out with design heat transfer area. (2) A 68% increase in the output over design value by the optimization carried out with increased heat transfer area. This report discusses the approach, methodology and results of the optimization study carried out. A simulator, MSFSIM which predicts the performance of a multi-stage flash (MSF) desalination plant has been coupled with Genetic Algorithm (GA) optimizer. Exhaustive optimization case studies have been conducted on this plant with an objective to increase the performance ratio (PR). The steady state optimization performed was based on obtaining the best stage wise pressure profile to enhance thermal efficiency which in-turn improves the performance ratio. Apart from this, the recirculating brine flow rate was also optimized. This optimization study enabled us to increase the PR of NDDP-MSF plant from design value of 9.0 to an optimized value 13.1. The actual plant is provided with 20% additional heat transfer area over and above the design heat transfer area. Optimization with this additional heat transfer area has taken the PR to 15.1. A desire to maintain equal flashing rates in all of the stages (a feature required for long life of the plant and to avoid cascading effect of non-flashing triggered by any stage) of the MSF plant has also been achieved. The deviation in the flashing rates within stages has been reduced. The startup characteristic of the plant (i.e the variation of stage pressure and the variation of recirculation flow rate with time), have been optimized with a target to minimize the startup time. The optimization was performed using MSFSIM startup coupled with GA optimizer. This study found the optimum path for the startup of control variables so that the plant reaches the steady state with PR of 15 in minimum time.

70	*Keywords/Descriptors :*	NUCLEAR POWER PLANTS; DESALINATION; OPTIMIZATION; DESALINATION PLANTS; PERFORMANCE; DESIGN; M CODES; VALIDATION; MATHEMATICAL MODELS; EVAPORATORS; BRINES; SEAWATER
71	*INIS Subject Category :*	S22
99	*Supplementary elements :*	

सारांश

NDDP-MSF संयंत्र के कार्यनिष्पादन अनुपात (PR) में उनके डिजाइन का 9.0 से 13.1 मान उपयुक्त प्रचालन अधिक्षेत्र की सीमा के अंदर संयंत्र के प्रचालन प्राचलों का इष्टतमीकरण प्राप्त किया गया था ।

1 डिजाइन ऊष्मा अंतरण क्षेत्र से इष्टतमीकरण द्वारा डिजाइन मान के ऊपर आउटपुट में 45% की वृद्धि ।

2 बढ़े हुए ऊष्मा अंतरण क्षेत्र के साथ इष्टतमीकरण द्वारा डिजाइन मान के ऊपर आउटपुट में 68 % की वृद्धि ।

रिपोर्ट में इष्टतमीकरण अध्ययन के दृष्टिकोण पद्धति एवं परिणामों की चर्चा की गई है ।

एक अनुकारक, MSFSIM, जो मल्टी स्टेज फ्लैश (MSF) निर्लवणीकरण संयंत्र के कार्यनिष्पादन का पूर्वानुमान लगाता है, को जेनेटिक एल्गोरिथ्म (GA) ऑप्टिमाइजर के साथ युग्मित किया गया । कार्यनिष्पादन अनुपात (PR) को बढ़ाने के उद्देश्य से संयंत्र पर संपूर्ण इष्टतमीकरण मामलों का अध्ययन किया गया । तापीय क्षमता को बढ़ाने के लिए स्थिर अवस्था इष्टतमीकरण कार्यनिष्पादन बेहतर चरण-वार दाब प्रोफाइल प्राप्त करने के आधार पर किया गया जिससे कार्यनिष्पादन अनुपात में वृद्धि होती है । इसके अलावा, रीसर्कुलेटिंग ब्राइन फ्लो रेट का भी इष्टतमीकरण किया गया । इस इष्टतमीकरण अध्ययन से NDDP-MSF संयंत्र के PR को 9.0 डिजाइन मान से 13.1 इष्टतमीकृत मान तक बढ़ाने में हमे सहायता मिली ।

वस्तुत: संयंत्र को डिजाइन ऊष्मा अंतरण अधिक्षेत्र के अतिरिक्त 20% अतिरिक्त ऊष्मा अंतरण क्षेत्र उपलब्ध कराया गया है । इस अतिरिक्त ऊष्मा अंतरण क्षेत्र के साथ इष्टतमीकरण से PR 15.1 तक पहुँच गया । MSF संयंत्र के सभी चरणों में समान फ्लैशिंग दर को बनाये रखने की इच्छा (संयंत्र की दीर्घायु एवं किसी भी स्तर द्वारा प्रेरित किए गए नॉन-फ्लैशिंग के केस्केडिंग प्रभाव को रोकने के लिए अपेक्षित एक लक्षण) भी पूरी हुई । चरणों के फ्लैशिंग दरों में विचलन को कम किया गया है ।

संयंत्र के स्टार्ट अप अभिलक्षण (अर्थात स्टेज प्रेशर में भिन्नता एवं समय के साथ रिसर्कुलेशन फ्लो रेट की भिन्नता), को स्टार्ट अप समय को न्यूनीकृत करने के लक्ष्य हेतु इष्टतमीकृत किया गया । GA ऑप्टिमाइजर के साथ युग्मित MSFSIM स्टार्ट अप का प्रयोग करते हुए इष्टतमीकरण किया गया ।

इस अध्ययन से नियंत्रण वेरियेवल्स के स्टार्ट अप हेतु मार्ग पथ प्राप्त किया गया ताकि संयंत्र निम्नतम समय में 15 के PR सहित स्थिर अवस्था में आ सके ।

Abstract

The improvement of NDDP-MSF plant's performance ratio (PR) from design value of 9.0 to 13.1 was achieved by optimizing the plant's operating parameters within the feasible zone of operation. This plant has 20% excess heat transfer area over the design condition which helped us to get a PR of 15.1 after optimization. Thus we have obtained,

1. A 45% increase in the output over design value by the optimization carried out with design heat transfer area.
2. A 68% increase in the output over design value by the optimization carried out with increased heat transfer area.

This report discusses the approach, methodology and results of the optimization study carried out.

A simulator, MSFSIM which predicts the performance of a multi-stage flash (MSF) desalination plant has been coupled with Genetic Algorithm (GA) optimizer. Exhaustive optimization case studies have been conducted on this plant with an objective to increase the performance ratio (PR). The steady state optimization performed was based on obtaining the best stage wise pressure profile to enhance thermal efficiency which in-turn improves the performance ratio. Apart from this, the recirculating brine flow rate was also optimized. This optimization study enabled us to increase the PR of NDDP–MSF plant from design value of 9.0 to an optimized value 13.1.

The actual plant is provided with 20% additional heat transfer area over and above the design heat transfer area. Optimization with this additional heat transfer area has taken the PR to 15.1. A desire to maintain equal flashing rates in all of the stages (a feature required for long life of the plant and to avoid cascading effect of non-flashing triggered by any stage) of the MSF plant has also been achieved. The deviation in the flashing rates within stages has been reduced.

The startup characteristic of the plant (i.e. the variation of stage pressure and the variation of recirculation flow rate with time), have been optimized with a target to minimize the startup time. The optimization was performed using MSFSIM startup coupled with the GA optimizer.

This study found the optimum path for the startup of control variables so that the plant reaches the steady state with PR of 15 in minimum time.

Contents

Chapter Number	Description	Page Number
	Title page	1
	Bibliographic sheet	3
	Abstract in Hindi	5
	Abstract	6
	Contents	7
1	Introduction	9
2	Validation and Problem Definition	10
3	Optimization using Genetic Algorithm - Steady State Simulation	16
4	Changed scenario in the NDDP-MSF desalination plant and its optimization	32
5	Startup optimization using GA	37
6	Conclusions and Future scope	42
	Nomenclature	44
	Acknowledgments	45
	References	45
	Appendix –A	47
	Appendix –B	50

Chapter 1
Introduction

A nuclear desalination demonstration plant (NDDP) is under construction at Kalpakkam, Tamil Nadu, India, with a design capacity of 4500m^3/day. A pilot plant of 425 m^3/day capacity was constructed, commissioned and successfully run at Desalination Division of Bhabha Atomic Research Centre, Trombay, Mumbai, in order to understand the process of nuclear desalination. Performance ratio is defined as the ratio of potable water produced per kilogram of steam consumed. The NDDP-MSF plant was designed based on the experience of this pilot plant [1-2]. A numerical simulator (MSFSIM) was developed at Machine Dynamics Division, based on mathematical modeling to aid the control systems in the plant [1,3-6]. This has features for troubleshooting and can aid in the training of the operators. This simulator was validated using the pilot plant data. Optimization of the NDDP-MSF plant is carried out for two purposes

1) Maximization of performance ratio (PR) and
2) Minimization of variation of flashing rates in all the stages.

In this report the optimization of parameters in the NDDP MSF plant to enhance its performance ratio has been discussed. MSFSIM has been coupled with the Genetic Algorithm optimizer. The primary parameters like 1) the stage wise pressure profile and 2) the recirculation flow rate are parameterized while the secondary parameters like reject and blow down are adjusted by the simulation code, MSFSIM so as to maintain thermal and concentration balance. The best operating parameters have been reported.

The steady state reached by the MSF plant is dependent on the path which the control variables have passed by during the startup of plant. It is equally important to reach the optimized steady state. Here we chose to minimize the time of startup. The startup characteristics of control variables 1) stage wise pressure variation with time and 2) recirculation flow rate variation with time were optimized. A differential error in the optimum control values should not yield in large change in the output of the plant. Again it is left to the decision of the instrumentation and control personnel of the plant how close can they operate to the optimum proposed in this report. The maximum possible PR has been reported. Also the best characteristics of the control variables are reported, so that the startup takes minimum time.

Chapter 2 of the report discusses the mathematical modeling and validation with respect to the pilot plant. Chapter 3 gives the details of the optimization study and elaborates the results suggesting the optimal zone of operation. Chapter 4 optimizes the changed scenario of the upcoming plant. Chapter 5 gives the details of startup optimization, followed by the future scope and conclusions.

Chapter 2
Validation and Problem Definition

The NDDP-MSF plant consists of a brine heater and 39 evaporators which are arranged in series. The flow sheet in Fig. 2.1 shows the arrangement of evaporators in the recovery and the reject stages for the NDDP-MSF plant. Fig. 2.2 gives the flow diagram for a typical brine evaporator.

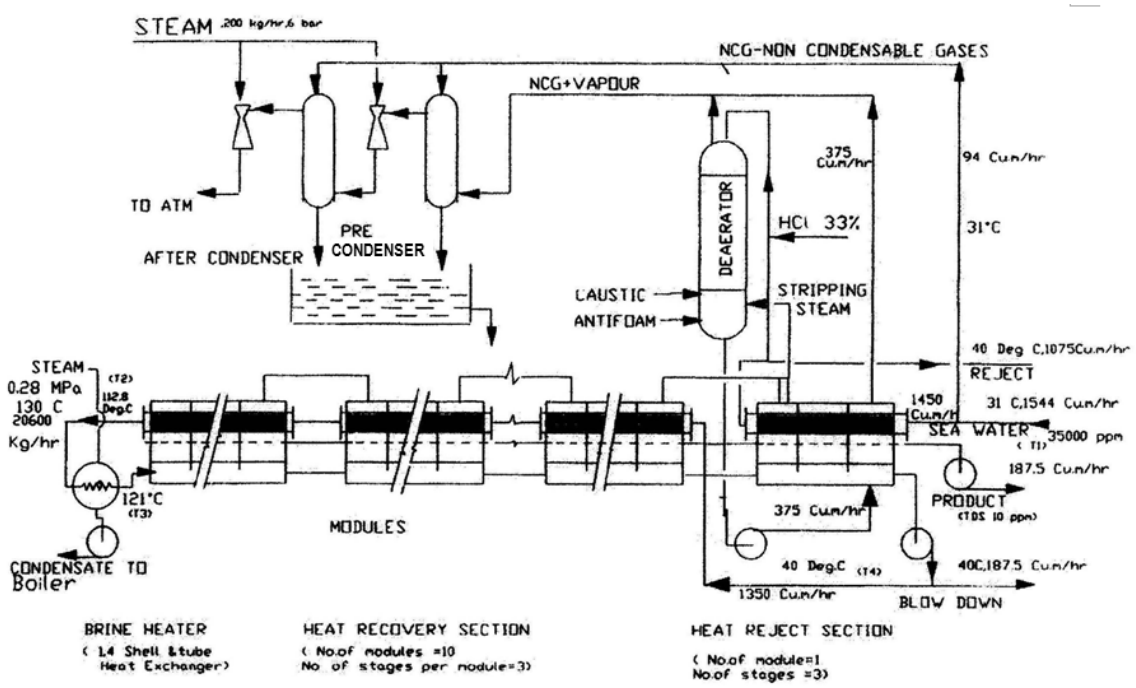

Figure 2.1 NDDP –MSF desalination flow sheet with design rating 4500m^3/day

Multistage flash desalination process can be described by a system of ordinary differential equations (ODE's) mentioned in the Appendix -A. Dynamic model equations were used so that steady state and transient (start up) can be modeled with the same set of equations. The correlations used for physical properties like density, viscosity, etc. of the brine are listed in the Appendix - A. Further details can be had from reference [6,7].

Steam table has been coded and used to determine the properties of the vapor. The steam supplied to the brine heater was taken as saturated. The thermal efficiency of the flashing chamber is assumed to be 99%. Non-equilibrium allowance has been given to the system [8]. It is also assumed that the vapor in the evaporator attains equilibrium with the liquid in contact instantly. Steam flow rate to the brine heater is held constant during the study also the brine level inside the evaporators are taken equal to the weir height throughout the stage length.

The numerical simulator, MSFSIM solves the ODE's simultaneously using Runge Kutta(RK) - 4 time stepping. The steady state simulations use pseudo time stepping, with large time step to enhance faster convergence. Whereas in transient simulations explicit time marching was implemented in outer time cycle (after being stabilized with Gauss Seidel inner iterations). For utilizing this simulator for training purpose, a graphic user interface (GUI) was also developed [5,6]. Appendix-B discusses the GUI encountered by the user for startup simulation. The MSFSIM code was extensively validated with the data of 425 m^3/day capacity pilot plant located at Trombay, Mumbai. This pilot plant has 30 recovery stages and 3 reject stages. The process details of the pilot plant are listed in Table 2.1 [5,6].

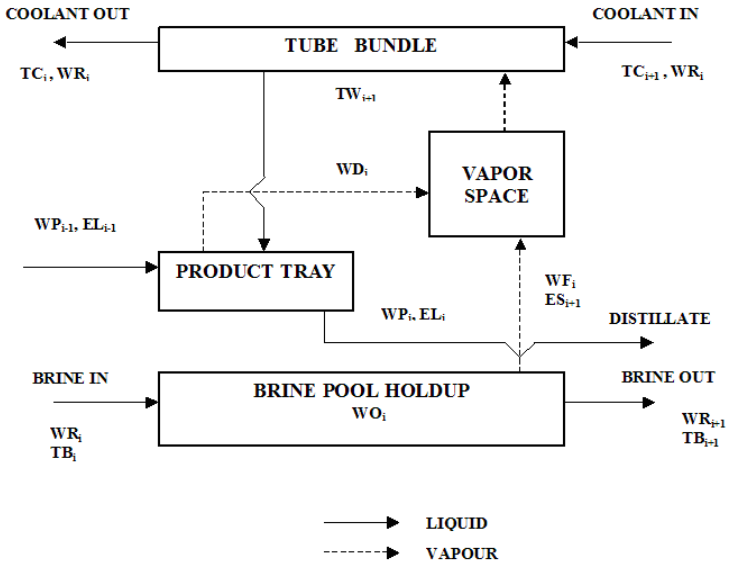

Figure 2.2 Flow diagram for a typical i^{th} evaporator

2.1 Validation with pilot plant data

The data from the pilot plant under normal operating conditions are compared with the simulated data from MSFSIM in Table 2.2. Fig. 2.3 and 2.4 shows a comparison of temperatures and production rate under startup condition with the pilot plant data. A time step of 0.01 minute was used in the numerical calculation. For further details please refer [5,6]. The systems of equations to be tested were given an impulse and step inputs and the stability of the solver were tested. The inputs tested were recirculation flow rate, steam mass flow rate / temperature, pressure in a few stages and salinity of sea water / temperature. The solver has converged for all the cases for which the tests were conducted. The numerical residue in the material and energy balance of the code is of the order of 10^{-4} %. Fig. 2.5 and 2.6 shows step inputs of steam and recirculation flow rates and their responses from NDDP-MSF plant simulator.

Table 2.3 gives the cross-correlation coefficient as well as the least squares error for brine heater inlet, outlet and the production rate in comparison with the experimental data as shown in Fig. 2.3 and Fig. 2.4.

Table 2.1 Process parameters of pilot plant at Trombay and NDDP-MSF at Kalpakkam

Parameters	***Pilot plant at Trombay***	***NDDP-MSF plant at Kalpakkam***
Distillate production rate (m^3/day)	425	4,500
Number of recirculation / reject stages	30 / 3	36 / 3
Feed water flow rate (m^3/hr)	90.5	1,544
Brine heater inlet temperature (° C)	113.0	112.8
Brine heater outlet temperature (° C), TBT	121.0	121.0
Performance ratio	9.0	9.0
Blow down salinity (ppm)	52,000	70,000
Blow down flow rate (m^3/hr)	35.0	187.5
Blow down temperature (°C), BBT	44.0	40.0
Rejection flow rate (m^3/hr)	38	1,075
Rejection temperature (°C)	40	40

Table 2.2 Comparison of the simulated data with the pilot plant data

Parameters	**Pilot Plant Data**	**Simulated by MSFSIM**
Distillate production rate (m^3/day)	425	430.52
Brine heater inlet temperature (° C)	113	114.07
Brine heater outlet temperature (° C), TBT	121	121.3
Performance ratio	8.92	9.03

It can be seen that MSFSIM compares well with the pilot plant data. Having validated the MSFSIM process simulator, the process optimization was carried out, as discussed in next chapter.

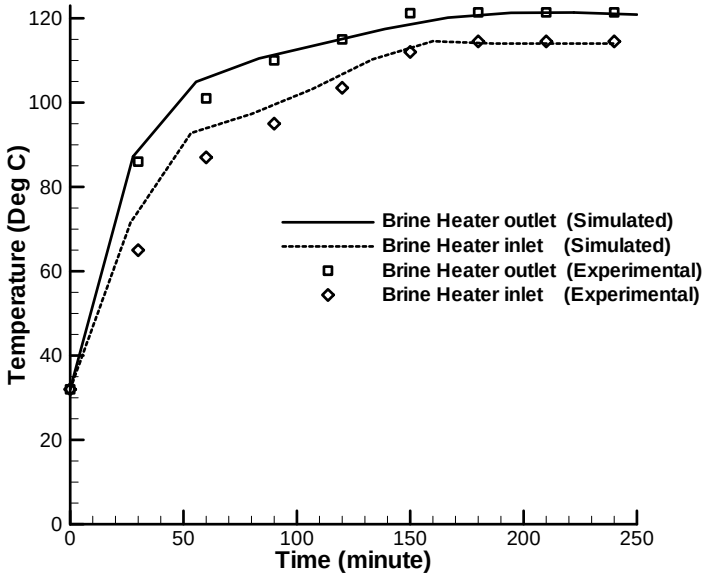

Figure 2.3 The development of brine heater temperatures compared with pilot plant data

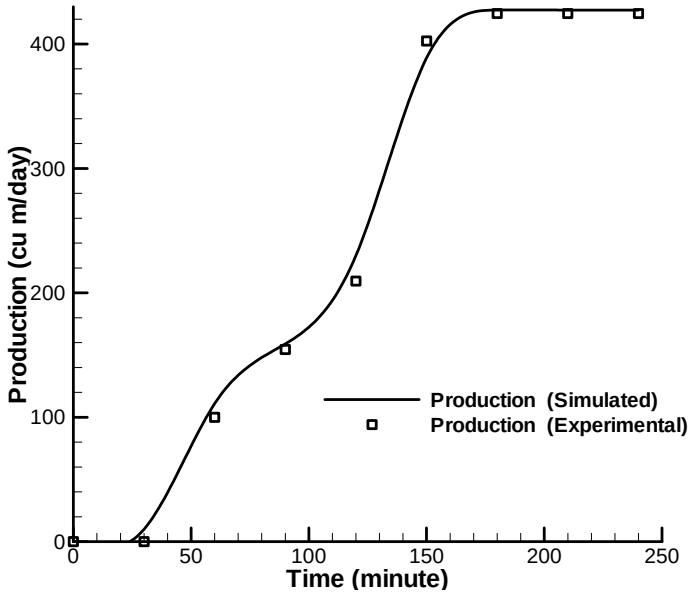

Figure 2.4 The production rate compared with pilot plant data

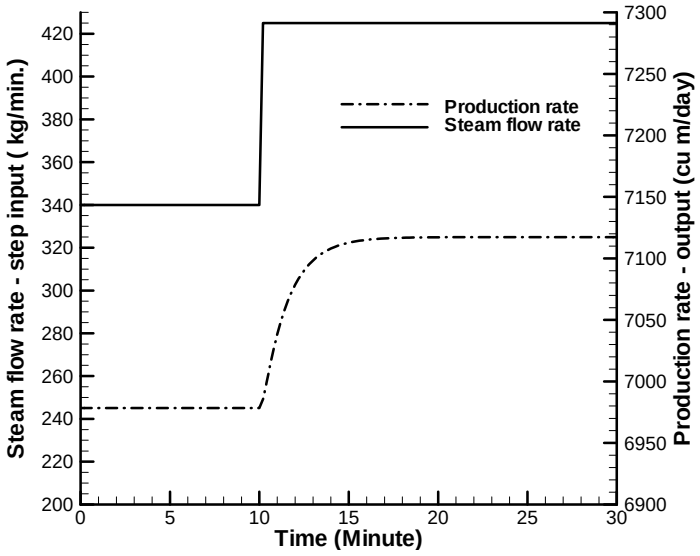

Figure 2.5 The response of production rate for a step input in steam flow rate in NDDP-MSF plant.

Table 2.3 Comparison of the startup with the experimental data

Parameter	***Cross correlation coefficient***	***Least Squares error***
Brine heater inlet temperature. Figure 2.3	0.9913	5.53 %
Brine heater outlet temperature. Figure 2.3	0.9972	2.46 %
Production rate (m^3/day) Figure 2.4	0.9988	4.87 %

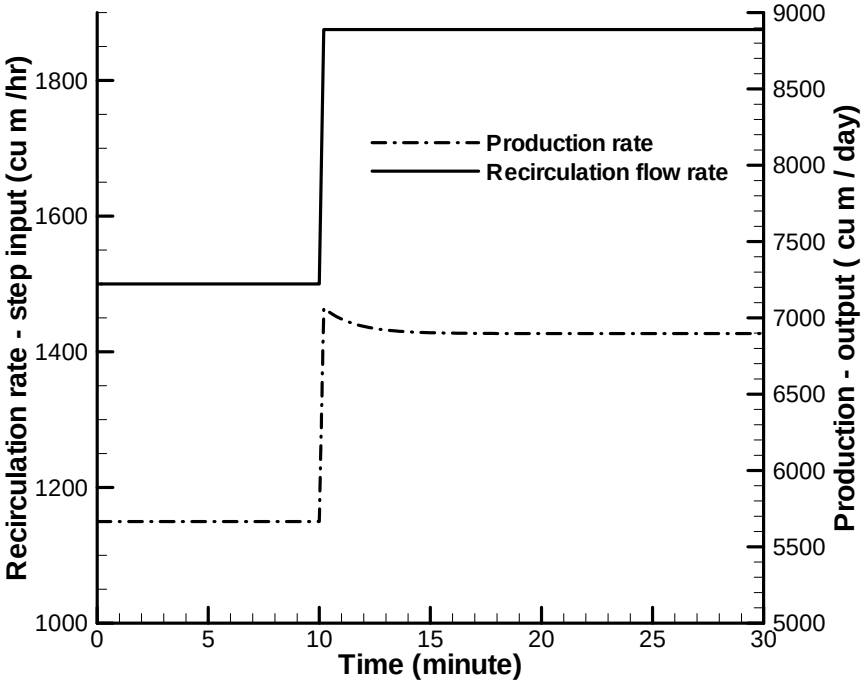

Figure 2.6 The response of production rate for a step input in recirculation flow rate in NDDP-MSF plant.

2.2 The performance of NDDP –MSF plant at the design condition

The accuracy and validity of MSFSIM (steady state and startup) solvers can be seen from the above mentioned validation of MSFSIM against the pilot plant data. The performance of the NDDP-MSF plant using MSFSIM was predicted. This plant contains 39 stages (36 recovery, 3 reject), with brine concentration ratio (BCR) operating at 2.0. BCR is the ratio of blowdown salinity to feed water salinity. The design velocity for the recirculating brine in stage number 1 was fixed at 1.2 m/s [2], thus the recirculating brine flow rate is fixed at 1,350 m^3/hr. Fig. 2.7 gives the flashing rates in all the stages under design condition for NDDP-MSF plant. The process details of the NDDP-MSF plant are listed in Table 2.1 [5,6].

2.3 Motivation for optimization

Variation of recirculation flow rate reveals the non-optimality of the design data. An increase in recirculating brine (here onwards referred as RB) flow rate alone increases the PR from design value of 9.0 as reported in [2] to 10.81. Flashing is very strongly dictated by the stage pressures. Optimal variation of stage pressure not only increases PR but can also minimize the variation amongst stage flash rates.

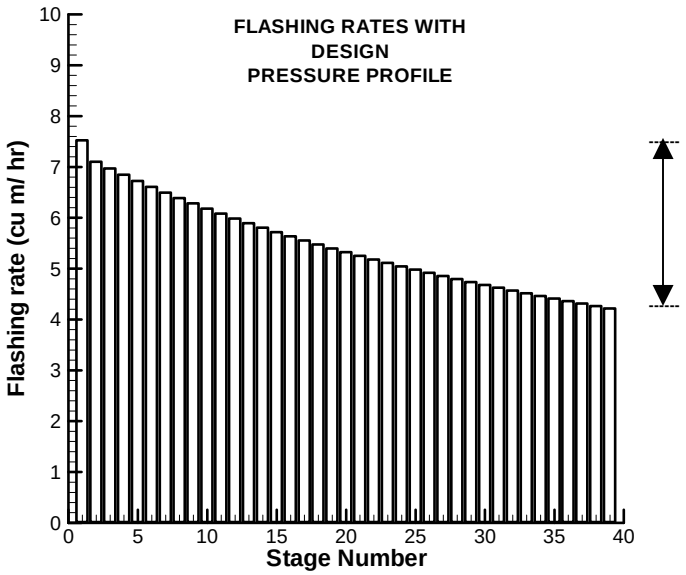

Figure 2.7 Stage wise flashing rates at design condition

Equal flashing in all stages is a desired feature for having a long sustained running of the plant and to avoid cascading effect of non-flashing triggered by any stage. But design condition does not provide this. It gives an average deviation of 0.8935m^3/hr from the mean value of flashing rate as shown in Fig. 2.7.

Definitely a better optimum should exist for this plant in terms of the operating conditions. The parametric space of feasible zone has been explored for reaching the optimum.

Chapter 3
Optimization using Genetic Algorithm - Steady State Simulation

Genetic algorithms are search algorithms based on natural selection and genetics. They combine survival of the fittest among the string structures with a structured yet randomized information exchange. In every generation, a new set of strings is created using bits and pieces of the fittest individuals of the older generation, an occasional new part is tried to maintain diversity. They efficiently exploit historical information to improve the performance [9].

3.1 Problem definition and optimization procedure

The optimization in this context requires maximization of PR (Performance Ratio) and minimization of average variation of the flashing rates (m^3/hr), σ in all the stages, defined as $\sigma = \left[\frac{1}{2}\sum_{i=1}^{39}(f_i - \bar{f})\right]^{1/2}$, f_i is the flashing in stage i and $\bar{f}$ is the average flashing in all stages. An optimization problem can be mathematically stated as follows :

Find

$$\vec{x} = \begin{bmatrix} x_1 \\ x_2 \\ \\ x_n \end{bmatrix} \in R^n \text{ which maximizes/minimizes Objective Vector } OF_i(\vec{x}) \in Y \in R^m$$

subject to constraints

Inequality	$g_j(\vec{x}) < 0$	$j = 1,2,..,m$	$\in R^l$
Equality	$h_k(\vec{x}) = 0$	$k = 1,2,..,p$	$\in R^l$
Goal Vector	$q(\vec{x}) \in Q$		$\in R^m$

(3.1)

where $\vec{x}$ is an n-dimensional design/control vector. In the present case the vector space is the stage pressures and the brine recirculation flow rate of a MSF plant, i.e. this vector space $\vec{x}$ =[P_1, P_2, ..,P_{39}, *Recirculation Brine flow rate*]^T. The first step is the parameterization of the design/control vector and the second most important step is to condense this vector space to a smaller dimensional space. The pressure profile variation is non-linear with respect to stage whereas the *Ts*, saturation temperature varies quite linearly with respect to stage. Thus, saturation temperature, *Ts* curve is parameterized instead of the stage pressure. The vector space is further condensed by fitting a cubic spline with the seven control parameters.

The inequality constraint defines the operating region of the designed plant. They are TBT $\leq$ 121°C, BBT $\geq$ 40°C, $f_i \geq 0.0$, 1.0m/s $\leq V_{RB,Max} \leq$ 1.6 m/s and S_{BD} = 70,000ppm. This can be casted into a vector format as follows.

$$g(\bar{x}) \equiv \begin{bmatrix} \text{TBT} - 121^{\circ}\text{C} \\ 40^{\circ}\text{C} - \text{BBT} \\ -\text{f}_\text{i}, \text{i} = 1,2,...,39 \\ |\, \text{V}_{\text{RB,Max}} - 1.3\,| - 0.3\text{m/s} \end{bmatrix} < 0 \quad \text{and} \quad h(\bar{x}) \equiv \left[S_{BD} - 70{,}000\, ppm \right] = 0 \qquad (3.2)$$

where $V_{RB,Max}$ is the maximum velocity of the recirculating brine inside the tubes and S_{BD} is the blow down salinity. The pumping limits of various pumps in the circuit gets determined by the limits of $V_{RB,Max}$.

Any change in the recirculation flow rate affects the reject, blow-down and sea water inlet flow rates. The optimization zone is within the pumping capacities of the installed pumps. The parameter of much concern to us is the maximum velocity of brine inside the tubes. If the maximum velocity in brine tubes is within the permissible limits (limits decided as per salinity to minimize fouling, $CaSO_4$ deposition). The stage pressure is bounded between the pressure in the first stage based on the TBT and the last stage based on the BBT. Hence the intermediate stage pressures are optimized.

One of the important task is to design an appropriate (i) parameterization, (ii) binary coding of parameter set, (iii) objective functions that can evolve to the global optimum using Genetic Algorithm (GA) and (iv) ability to find multiple Pareto-optimal solution in a single run. An inappropriate handling of constraints may lead to a local optimum of the problem. It should be noted that stability of optimization is also of equal concern. This requires construction of the Jacobian at the optimal point and its Eigen-values, if real part is negative the optimal point is stable.

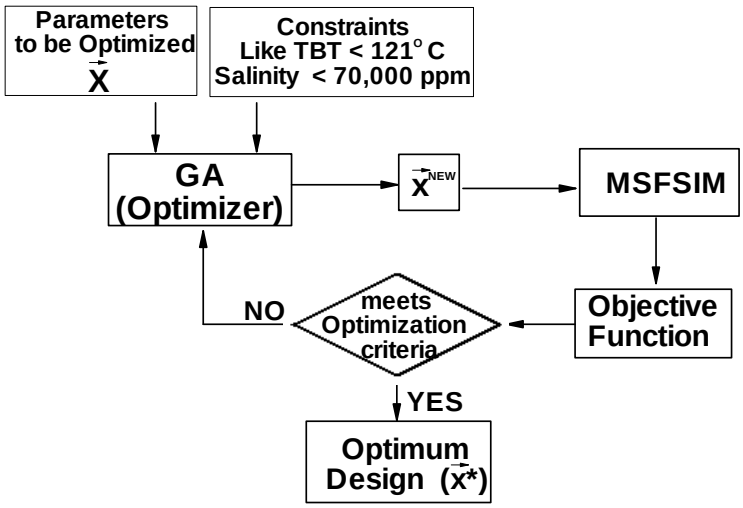

Figure 3.1 Schematic of the GA-MSF optimizer

See Fig. 3.1 for a schematic of the optimization study. An optimization study using downhill simplex method was tried earlier. The optimum obtained using this method was always very close to the initial guess chosen and good increase in objective

function was not achieved. Probably the method gets stuck in the local optimum close to the initial guess. It was decided to try a population based method to get a global optimum. There are many population based methods namely Simulated Annealing (SA), Genetic Algorithm (GA), ANT algorithms, etc. Out of these GA and SA have been extensively reported for determining the Pareto set of optimization. Earlier experience with GA [11-13] has made it the obvious choice for this problem. GA searches from multiple vectors in the design space simultaneously and stochastically, instead of moving from a single point deterministically like in gradient-based methods. This feature prevents optimal candidates from settling in local optimum. Moreover, GA does not require computing gradients of the objective function [10-13]. These characteristics lead to following three advantages of GA:

i) GA has capability of finding global optimal solutions.

ii) GA can be processed in parallel.

iii) MSF design and analysis codes can easily be adapted to GA without any modification because GA uses only objective function values.

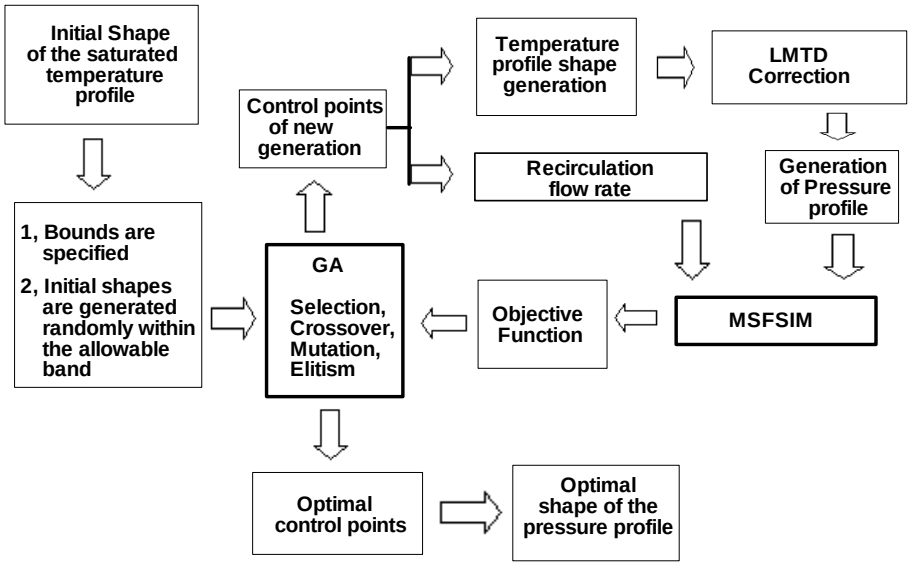

Figure 3.2 The schematic showing the procedure of coupled MSFSIM with GA

Fig. 3.2 shows the schematic of the procedure used for coupling MSFSIM with GA. GA works on a coding of the design variables subject to the defined performance constraints.

Fig. 3.3 shows a typical chromosome structure. It contains of 9 parameters, each coded as 15 bit binary code and concatenated to form a single string. Fig. 3.4 shows a typical saturated temperature (*Ts*) profile in various stages. The stage pressure is determined as a function of *Ts*. The *Ts* curve is parameterized as shown in Fig. 3.4. As explained earlier, this is achieved by fitting a cubic spline with seven control parameters. Cubic spline with seven control parameters do not regress the saturated temperatures of the 39 stages. Here it is used to ensure inter stage smoothness, otherwise there can be drastic jumps and discontinuities in saturated temperature between stages. Such a discontinuous pressure / temperature profile lead to unrealistic / unimplementable conditions. In order to meet the 1st constraint of top brine temperature (TBT) < 121^{o}C;

saturated temperature for 1st stage is taken to be constant at 117.2°C. The vacuum system available in this plant has a constraint on bottom brine temperature (BBT) > 40°C, Thus, the saturated temperature for the 39th stages was chosen to be constant 39.5°C.

Parameter Number	Binary code of 1st parameter	Binary code of 2nd parameter
1, 2	1 0 0 1 1 0 0 1 1 0 1 0 1 0 0	0 0 0 1 0 1 1 0 0 1 1 1 0 1 1
3, 4	0 0 1 0 0 0 1 1 0 0 1 0 1 0 0	1 1 1 0 0 1 0 0 1 1 0 0 0 0 1
5, 6	0 0 1 1 1 1 1 1 0 1 1 0 1 0 0	0 1 1 1 1 0 0 0 0 0 0 1 1 0 0
7, 8	1 0 1 1 0 0 0 1 1 1 0 1 0 0 1	0 0 1 0 1 1 0 0 0 1 0 0 0 0 0
9	0 1 0 1 0 1 1 1 0 0 1 0 1 0 1	

Figure 3.3 A typical chromosome for the control parameters chosen

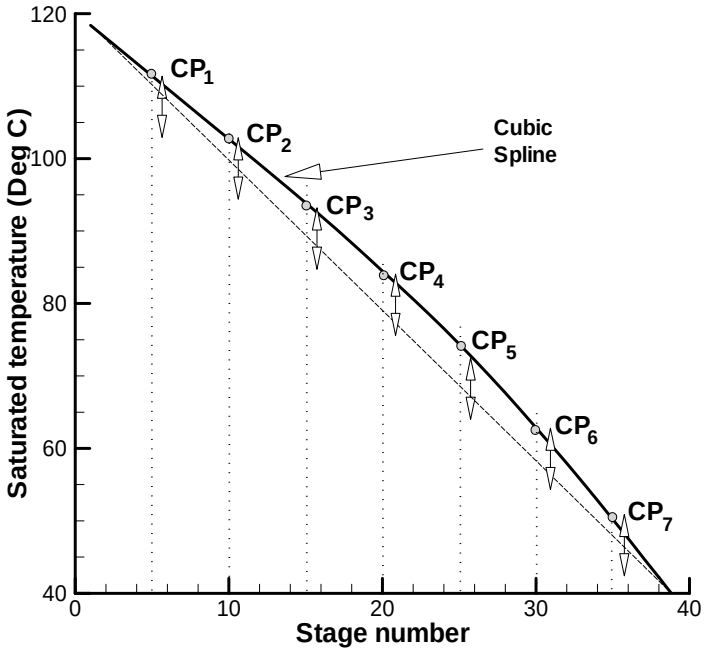

Figure 3.4 A typical curve showing the temperature vs. stage number plot.

Each of the 7 control points (CP_i) for the *Ts* curve vary as the percentage of the initial (design) value (see Fig. 3.4). Even though spline smoothens the inter stage saturated temperature, but in real life there are small discrete jumps in the inter stage saturated temperatures. Numerically the correction based on log mean temperature difference (LMTD) is introduced to bring a local discreteness in the saturated temperature profile.

Fig. 3.5 shows a typical temperature profile of recirculating brine in a stage. A change in pressure profile and recirculating flow rate leads to change in LMTD in all the stages. It should be noted that for higher values of LMTD the performance improves. Any correction for the *Ts* curve based on the LMTD at a fixed recirculation flow rate will change the vapor space temperature thereby fixing the stage pressure. The value of *Ts* for each stage is readjusted using the following equation.

$$T_s\big|_{\text{Stage i}} = T_s\big|_{\text{Stage i}}^{\text{From spline}} + \left[\text{LMTD}\big|_{\text{Mean}}^{\text{Reference}} - \text{LMTD}\big|_{\text{Stage i}}^{\text{Reference}} \right] \times \frac{\text{LMTD}\big|_{\text{Stage i}}}{\text{LMTD}\big|_{\text{Mean}}} \times \Psi \quad (3.3)$$

This adjusts the stage pressure such that the LMTD of each stage approaches the mean LMTD. The Ψ - factor brings the discreteness in the stage pressure profile. This forms the 8th parameter in the optimization process. The LMTD for all the stages are calculated and stored for the elite member in the previous generation. This forms the reference set for $LMTD_{Mean}$ and $LMTD_{Stage\ i}$. The 9th parameter used in this optimization is the recirculation flow rate. In this analysis, a given population represents a number of configurations with different *Ts* (or) pressure profiles, a factor for LMTD correction and various recirculation flow rates. Thus each configuration is regarded as a single chromosome. The initial guess of the control parameters is randomly generated. All the parameters are allowed to vary within a band as shown Fig. 3.6 and 3.7. The population size is set to 16. The Fitness evaluation is the basis for GA search and selection procedures. GA aims to reward individuals (chromosomes) with high fitness values (more fit for reproduction) and to select them as parents to reproduce off-springs. The purpose of optimization in this study is to increase the performance ratio of the MSF plant.

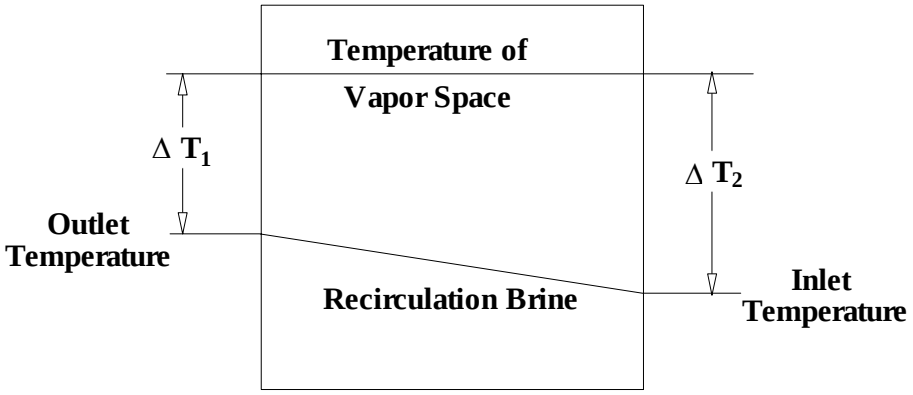

Figure 3.5 Typical recirculating brine temperature profiles

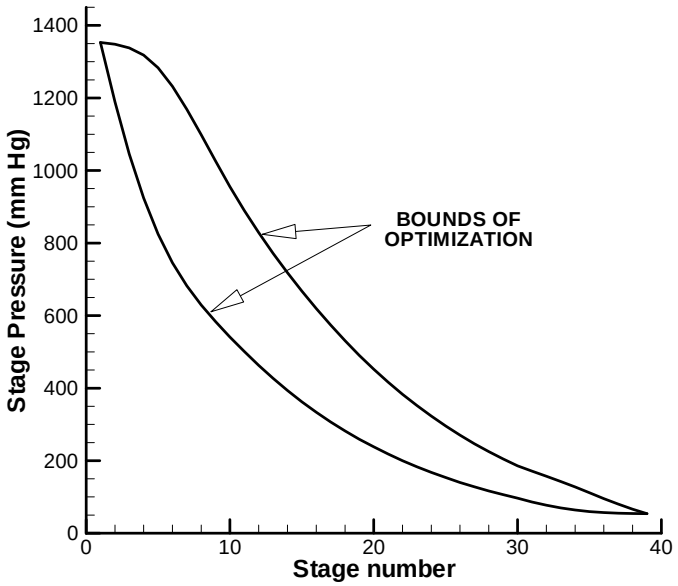

Figure 3.6 The search space for the optimization of pressure profile

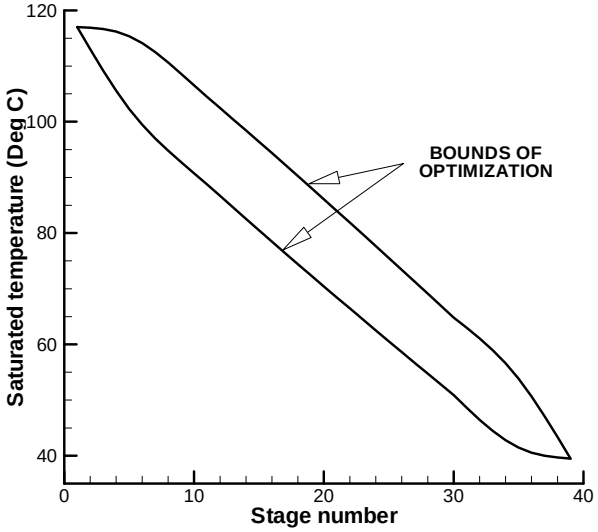

Figure 3.7 The search space for the optimization of Ts profile

3.2 Multi-Objective Function Optimization

3.2.1 Introduction to multi-objective optimization

There are multiple objectives, multiple constraints. The concept of Pareto optimality has been taken as the basis for the cooperative multiple objective optimization. This uses the dominance strategy where an optimum $\vec{x}^*$ is said to dominate $\vec{x}$ if and only if

$$\begin{cases} \forall\, i \in \{1,2,...\mathrm{n}\}, \mathrm{OF_i}(\vec{x}^*) \le OF_i(\vec{x}) \\ \exists\ i \text{ such that } \mathrm{OF}_i(\vec{x}^*) < OF_i(\vec{x}) \end{cases} \tag{3.4}$$

This $\vec{x}^*$ is said to be non-dominated if there is no feasible solution in the search space that dominates it. The Pareto front is a set of all such non-dominated solutions.

Most of the real life problems have multiple conflicting objective functions known as a multi-objective optimization problem. Any m-objective $(\mathrm{m} \ge 1)$ optimization problem can be described as in equation (3.1). There are multiple objectives, multiple constraints.

In the present case there are two objective functions : maximization of PR (Performance Ratio) and minimization of average variation of the flashing rates (m^3/hr). There is variety of commonly used methods[20] for multi-objective optimization. Three of the most commonly used methods can be stated as follows:

Method 1 : Sum of weighted objectives (MOGA by Murata *et al.*[17])

$$\text{minimize } f = \sum_i^m w_i f_i$$
$$\text{subject to } \vec{x} \in R^n; \text{ where } w_i > 0 \text{ and } \sum \mathrm{w_i} = 1 \tag{3.5}$$

Method 2 :Non dominated sorting

The objectives are treated independently. Ranking of objectives into "non-dominated order" with the fittest being the least dominated with a higher probability of having more offspring.

Method 3 : Increasing the constraint vector space

In this method one of the objective function is taken as the most primary and the remaining objective functions are transformed into constraints.

$$\text{minimize } f_1(\vec{x}) \text{ subject to } f_2(\vec{x}) \le c_2, ..., f_m(\vec{x}) \le c_m \ \vec{x} \in R^n;$$

where c_i is the bound

All these methods provide point solutions. Here parameter vector $\vec{\mathrm{x}}$ based on weights, objective value bounds, preferences based on experience, engineering judgment, etc. Trade-offs in optimum solutions over a wide range of weights can give a better picture. In such a scenario concept of Pareto optimality can be taken as the basis.

3.2.2 Pareto Optimality

In the present paper let us define optimization as a minimization problem as any maximization problem can easily be transformed to minimization problem. The concept of Pareto optimality has been taken as the basis for the cooperative multiple objective optimization.

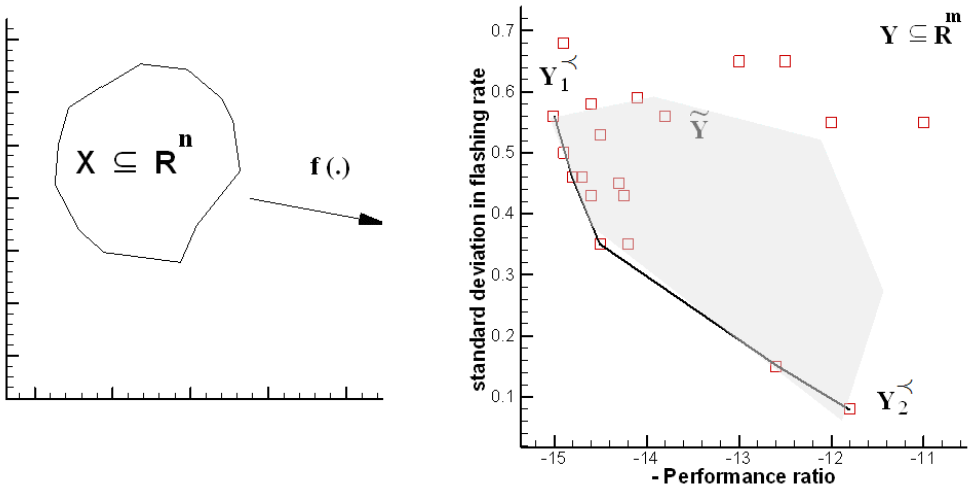

Figure 3.8 Mapping of the parameter space X to the objective function Y. $\tilde{Y}$ represents random points in the objective space and $\partial Y^{\prec}$ marks the Pareto optimal front bounded between $Y_1^{\prec}$ and $Y_2^{\prec}$.

This uses the dominance strategy where an optimum $\vec{x}^*$ is said to dominate $\vec{x}$ if and only if equation (3.3) is satisfied. This $\vec{x}^*$ is said to be non-dominated if there is no feasible solution in the search space that dominates it. The Pareto front is a set of all such non-dominated solutions. The concept of Pareto optimality can best be understood if we transform graphical solutions from n-dimensional parametric or design space **X** to m-dimensional objective or criterion space **Y**. The shaded region is the feasible region defined by the constraints and region marked as $\partial Y^{\prec}$ in figure 3.8 represents Pareto optimal front in the objective space.

Multi-objective genetic algorithms are developed based on two concepts called niching and Pareto-dominance. The Pareto-dominance is used to explore the search space in the direction of the Pareto front while niching explores the search space along the front to reach diversity. Pareto filter algorithm is employed to eliminate Non-Pareto or locally Pareto solutions. In the GA Pareto points and are identified and are mated together. Adjustments are made to the fitness values to avoid clustering.

Schaffer [14] proposed vector evaluated genetic algorithm(VEGA), Goldberg [15] suggested non-dominated sorting , Fonseca *et al.* [16] and Murata *et al.* [17] proposed multiple objective genetic algorithm (MOGA).Horn *et al.*[18] proposed niched-Pareto genetic algorithm (NPGA). Deb et. al. [19,20] proposed elitist non-dominated sorting genetic algorithm (NSGA-II). Multi-population genetic algorithm (MPGA) proposed by Cochran et. al. [21] combined the strengths of MOGA and VEGA. Each of these methods differed primarily on the basis of evaluating Pareto-optimal solutions. Hybrid method based on combination of GA and Ant Colony Optimization (ACO) [24] is also quite promising. GA based optimizer slows down as it reaches the global optima hence it is followed by Ant Colony Optimizer (ACO) to speed up the convergence. Research is going on to modify ACO for multi-objective optimization.

The method employed in this paper is similar to Deb[22] and Mahendra et. al. [23]. This method is essentially based on scalarizing function,

$$s : Q \times Y \rightarrow R^1 \tag{3.6}$$

The scheme for selecting the best solution along the Pareto front depends on the decision maker's or designer's overall preferences. Min-max optimization is generally used where selected Pareto point is chosen by minimizing its maximum deviation from the *ideal point* or the *demand point.* This is best illustrated in the following figure 3.9.

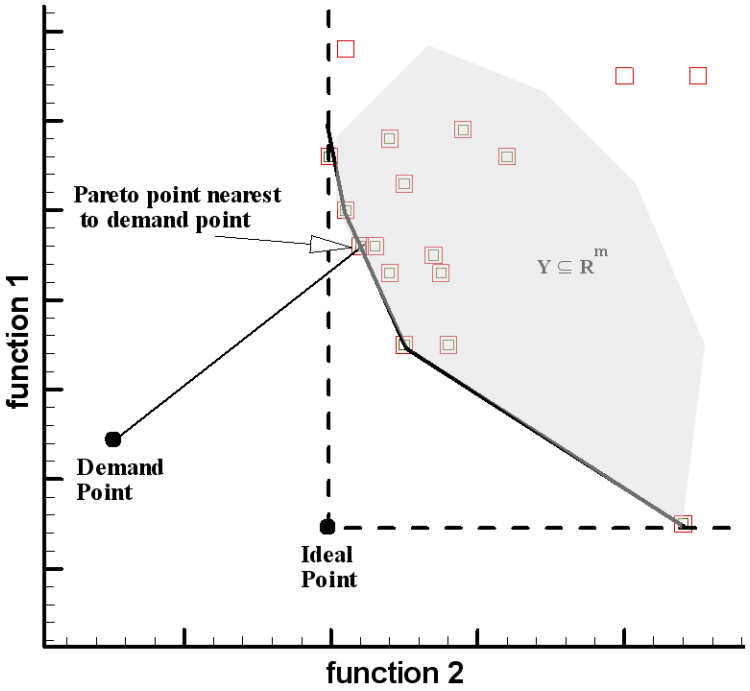

Figure 3.9 Pareto point nearest to the Demand point

Thus, the min-max optimization where maximum distance from either *demand point* or *ideal point* is minimized can be written as suggested by Mahendra *et al.*[23]

$$\min\left[\max\left\{\left|f_1(\vec{x})-y_1^{D*}\right|,\left|f_2(\vec{x})-y_2^{D*}\right|,...,\left|f_m(\vec{x})-y_m^{D*}\right|\right\}\right]$$

or (3.7)

$$\min\left[\max\left\{\left|f_1(\vec{x})-y_1^{I*}\right|,\left|f_2(\vec{x})-y_2^{I*}\right|,...,\left|f_m(\vec{x})-y_m^{I*}\right|\right\}\right]$$

Where the goal vectors are defined as $\vec{q} = \{y_1^{D*}, y_1^{D*}, ...y_m^{D*}\}$ (3.8)

Alternatively weighted Euclidean distance measure given by equation (3.7) can be minimized as suggested by Deb *et al.*[22]

$$d_{ij} = \sqrt{\sum_{i=1}^{m} w_i \left(\frac{f_i(\vec{x})-y_i^{D*}}{f_i^{\max}(\vec{x})-f_i^{\min}(\vec{x})}\right)^2} \quad \text{or}$$

$$d_{ij} = \sqrt{\sum_{i=1}^{m} w_i \left(\frac{f_i(\vec{x})-y_i^{I*}}{f_i^{\max}(\vec{x})-f_i^{\min}(\vec{x})}\right)^2} \tag{3.9}$$

The method of determining ranking is based on either distance from the demand point of the points chosen from the (i) non-dominated ranks or (ii) ranks based on ε-dominance [22] defined by the following equation

$$\vec{y}^* \prec \vec{y} :\Leftrightarrow \forall_{i\in\{1,2,..,m\}} (y_i^* \le y_i) \wedge \exists_{i\in\{1,2,..,m\}} (y_i^* < y_i - \varepsilon_i) \quad (3.10)$$

where $\varepsilon_i \in (0,1)$

ε_i based on the distance from the demand point. Here the niching as shown in Fig. 3.10 operates in the high rank zone, thus ensuring diversity in a larger non-dominated set near the demand point.

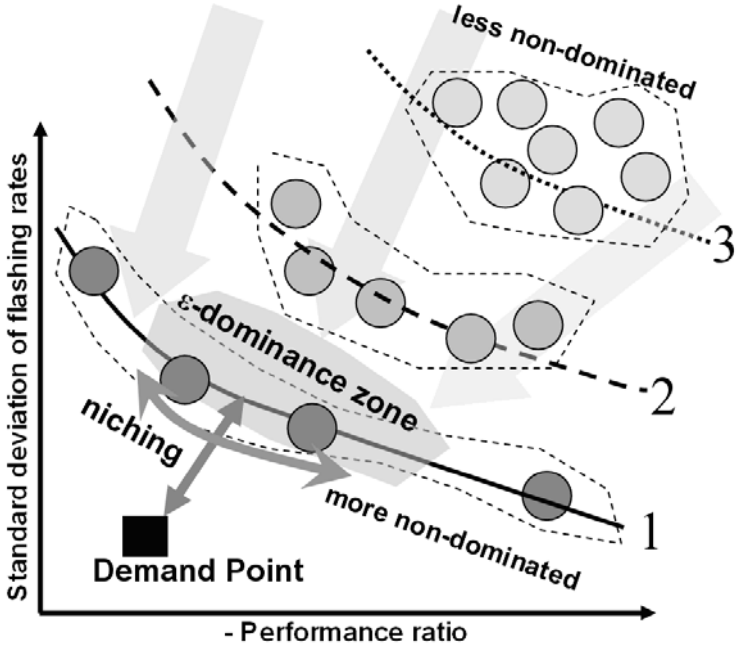

Figure 3.10 Niching based on demand point

This multi-objective function (*OF*) increases the *PR* as well as reduces the variation in flashing rates in all the stages. The MSFSIM calculates the *PR* with the pressure profile and recirculation rate provided and sends them to GA, which uses this formula to obtain the objective function (*OF*), which is a measure of fitness of that configuration (parameters).

Table 3.1 Initial input range for GA

Control Parameter	**Mean value**	**Range**
CP_1 (control point at stage=5)	108.84	-7% to 7%
CP_2 (control point at stage =10)	98.645	-8% to 8%
CP_3 (control point at stage =15)	88.447	-9% to 9%
CP_4 (control point at stage =20)	78.250	-10% to 10%
CP_5 (control point at stage =25)	68.053	-11% to 11%
CP_6 (control point at stage =30)	57.855	-12% to 12%
CP_7 (control point at stage =35)	47.658	-13% to 13%
CP_8 (Ψ - factor based on LMTD)	0.0	-30% to 30%
CP_9 (RB flow rate)	1463	-23% to 23%

The best members in each generation are assigned to the next generation without crossover or mutation [9,15]. This technique known as elitism, guarantees that the best member in all the populations will not be filtered out as the optimization proceeds. The optimization would continue till the *OF* vs. generation curve saturates. The highest *OF* contributing member would be our optimum solution to the problem.

3.3 Results and discussion

Our previous research experience using GA based optimizer [11-13] has helped in choosing the parameters that will be used within GA (Table 3.2). The details of the optimized sets of parameters are given in Table 3.3. Here PR reaches a value of 13.12 when the optimized recirculation flow rate is around 1795 m^3/hr.

Table 3.2 The parameters of GA

Population size	16
Max number of generation	130
Number of bits per parameter	15
Crossover probability	0.9
Jump mutation probability	0.2
Creep mutation probability	0.05
Elitism used	
Tournament selection used	
Uniform cross over used	

Fig. 3.11 shows a comparison between the design and optimized pressure profile. Fig 3.12 shows the flashing rates in various stages with optimized pressure and recirculation flow rates. Fig. 3.10 gives a comparison between the design pressure profile and the optimized pressure profile.

Table 3.3 Optimized parameters set obtained

Parameter	**Differential value**	**Actual value**
CP_1 (control point at stage=5)	2.36%	111.410
CP_2 (control point at stage=10)	5.54%	104.110
CP_3 (control point at stage=15)	7.35%	94.950
CP_4 (control point at stage=20)	8.38%	84.809
CP_5 (control point at stage=25)	9.55%	74.552
CP_6 (control point at stage=30)	9.51%	63.360
CP_7 (control point at stage=35)	6.03%	50.532
CP_8 (Ψ - factor on LMTD)	28%	0.28
CP_9 (RB flow rate)	21.3% to 22.7%	1775 to 1795
PR	12.86 to 13.12	

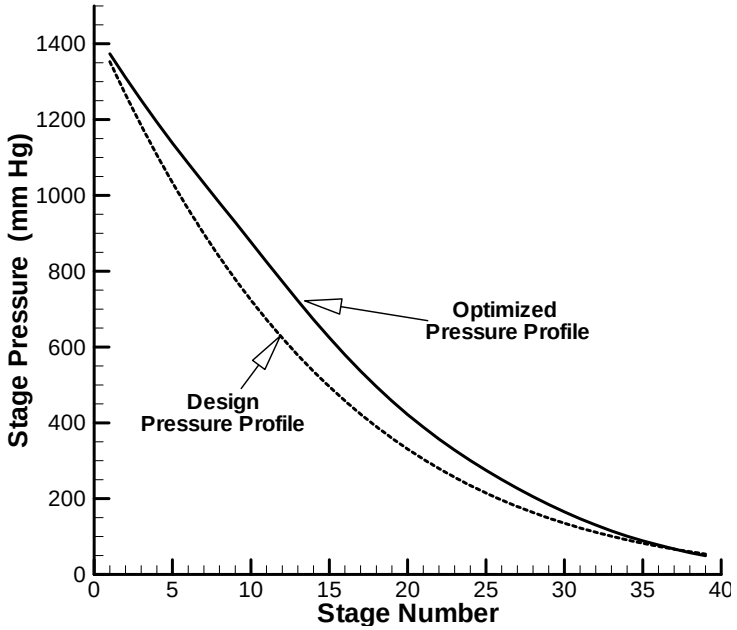

Figure 3.11 The comparison of optimized and design (initial) pressure profile.

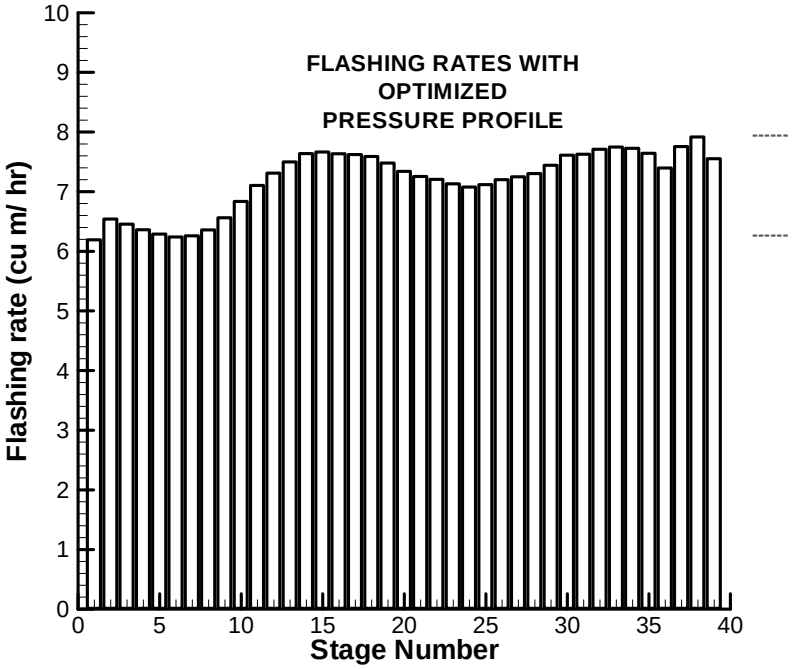

Figure 3.12 The flashing rates in stages under optimized condition

3.4 Possibility for optimum

The recirculating brine which gets preheated in the evaporator stages is the most critical part of the MSF plant which has a role to play in our optimum design. The log mean temperature difference (LMTD) for a given recirculating brine in each stage is calculated. The recirculation flow rate used is also higher in the optimized case. As

expected, the sum of LMTD in all the stages for optimized case is higher than the design case.

The Fig. 3.13 confirms our conclusion that LMTD in many stages has improved due to optimum pressure profile along with appropriate increase in recirculation flow rate. The average LMTD increases from 4.32 ^{o}C (design) to 5.08 ^{o}C (optimum case). Fig. 3.14 shows the comparison between design and optimum for recirculating brine inlet and outlet temperatures.

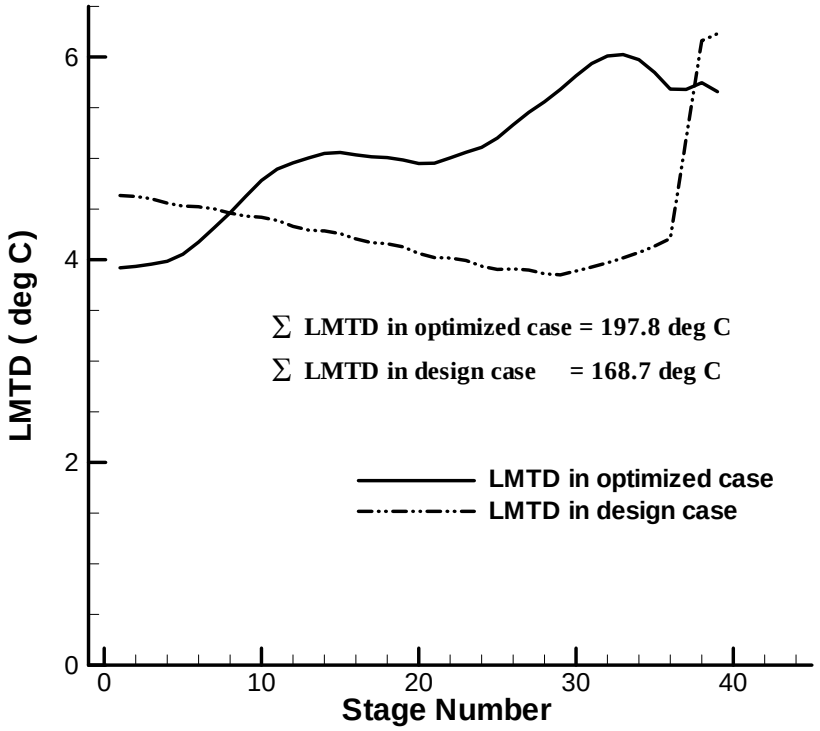

Figure 3.13 The LMTD for the design and optimized cases are shown for all stages.

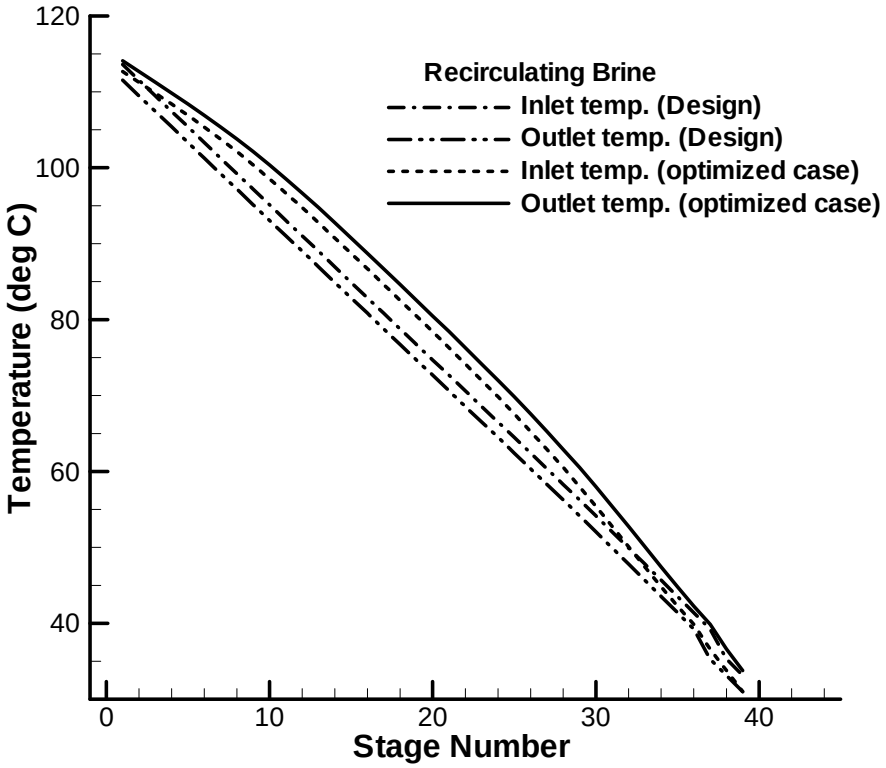

Figure 3.14 The inlet and outlet temperatures of the RB for design and optimized cases are shown for all stages

During the process of optimization the temperature of the vapor space changes as a consequence of the pressure change. Similarly an increase (or decrease) in recirculation flow rate changes the ΔT_1 and ΔT_2 as shown in Fig.3.5. Thus the optimum pressure profile and recirculation flow rates leads to a higher log mean temperature difference (LMTD) in all the stages. (i.e. higher $\sum_{i=1}^{39} LMTD$). Thus the temperature gained in the recirculation section is directly proportional to the $\sum_{i=1}^{39} LMTD$.

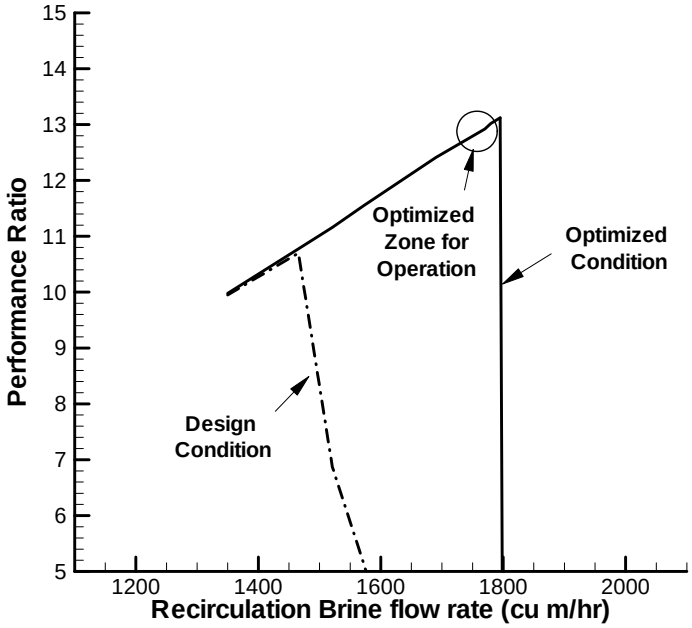

Figure 3.15 Comparison of PR vs. RB flow rate for design and optimized cases

Table 3.5 gives the details of the optimized condition in comparison with the design condition. Fig. 3.15 shows the comparison between design and optimum PR as a function of recirculating brine flow rate. It shows a sharp drop in PR when the RB flow rate crosses a threshold value. By optimizing the pressure profile there is an increase in the total LMTD of all stages i.e. $\sum_{i=1}^{39} LMTD$ which increases the value of Top Brine Temperature (TBT) for a given recirculation flow rate.

Table 3.4 Comparison of LMTD under design and optimized conditions

	Design condition	**Optimized condition**
$\sum_{i=1}^{39} LMTD$	168.7 ^{o}C	197.8 ^{o}C
RB flow rate	1350 m^3/hr	1785m^3/hr

In any MSF plant, the TBT keeps on decreasing with increasing in RB flow rate. When the TBT reduces below the 1st stage flashing temperature, there is no flashing in the 1st stage. This leads to a stoppage of flashing cascading to higher stages (like 2nd, 3rd, etc.). Thus the PR drops suddenly as the RB flow rate crosses this threshold RB flow rate. Fig 3.15 shows that the optimized pressure profile helps in increasing this threshold RB flow rate from 1,480 m^3/hr (with design pressure profile) to 1,795 m^3/hr(with optimized pressure profile). This increase in RB flow leads to higher value of PR of 13.11. At still higher RB flow rates the PR drops sharply due to non-flashing of stages. Thus, the stability of the plant around the optimum is also of equal concern. The operating optimum RB flow rate should be away from this "*non-flashing cliff*". The optimum RB flow rate should be chosen suitably far from this unstable location.

Table 3.5 The details of the optimized steady solution

Description	MSF at Design condition	MSF at Optimized condition
Capacity	4,500 m^3/day	6,485 to 6,590 m^3/day
Top brine temperature	121. °C	120.18 to 120.31 °C
RB flow rate	1,350 m^3/hr	1,778 to 1,792 m^3/hr
Brine heater temperature rise	8.2 °C	6.33 °C to 6.25 °C
Performance ratio	9.0	12.86 to 13.11
Average deviation of flashing in all stages	0.894	0.536 to 0.552

Chapter 4

Changed scenario in the NDDP-MSF desalination plant and its optimization

An additional 20% RB tubes have been provided for two reasons, namely,

1. to adjust itself to the seasonal variation of sea water temperature and
2. to meet the extra demand for water whenever needed.

The entire zone of RB flow rate from 1350 m^3/hr to 2000m^3/hr and heat transfer area from design value to the maximum available value which is 20% excess of design value has been scanned for evaluating the value of PR. This is shown as a contour plot in Fig. 4.1.

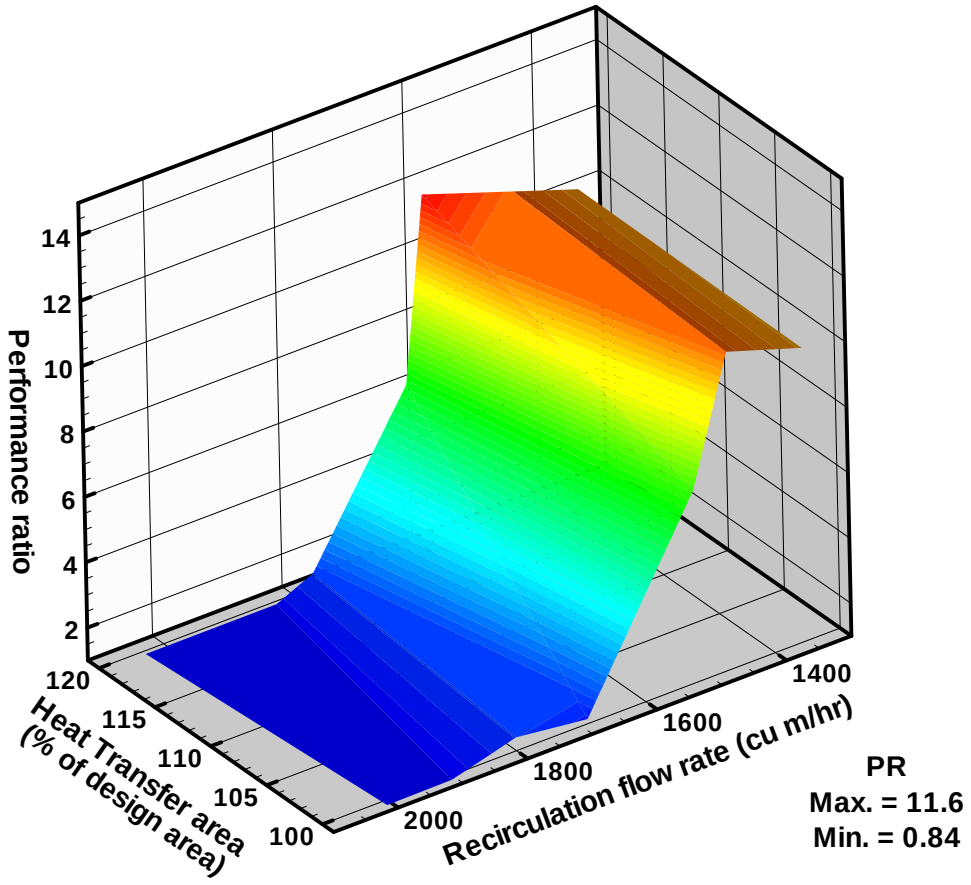

Figure 4.1 PR as a function of heat transfer area and RB flow rate at design pressure conditions

Thus an increase in area alone cannot increase the PR proportionately. A change in the operating heat transfer area always calls for an optimization study to decide the best operating conditions for the plant.

The details of the parameterization and the definition of objective function remain the same. However the limits of optimization have been changed. The region in

the vicinity (±4% to ±5%) of the optimum already obtained was chosen as our new design space as shown in Fig. 4.2. The initial condition used was the optimum obtained in section 3.3.

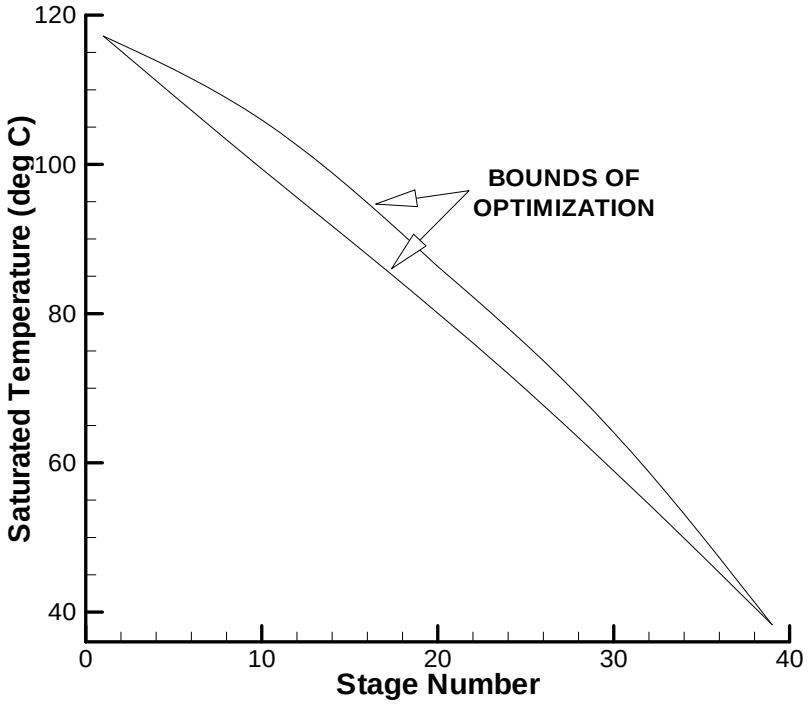

Figure 4.2 The search space for the optimization of pressure profile

Fig 4.3 shows the three demand points that were considered for the optimization study. Also Table 4.1 gives the comparison of the optimum obtained w.r.t the demand points. The demand point 1 was found to give us the most acceptable optimum. Fig. 4.4 gives the change in PR with the RB flow rate. A comparison of design and optimized pressure profile conditions are clearly shown. The GA based optimizer converges to an optimum in 19 generations, the details of the optimum is given in Table 4.2. A PR of 15.1 is obtained with our new optimized pressure profile when the recirculation flow rate is 2,085 m^3/hr. Fig. 4.4 gives a comparison of optimized pressure profiles under design and 20% excess heat transfer area.

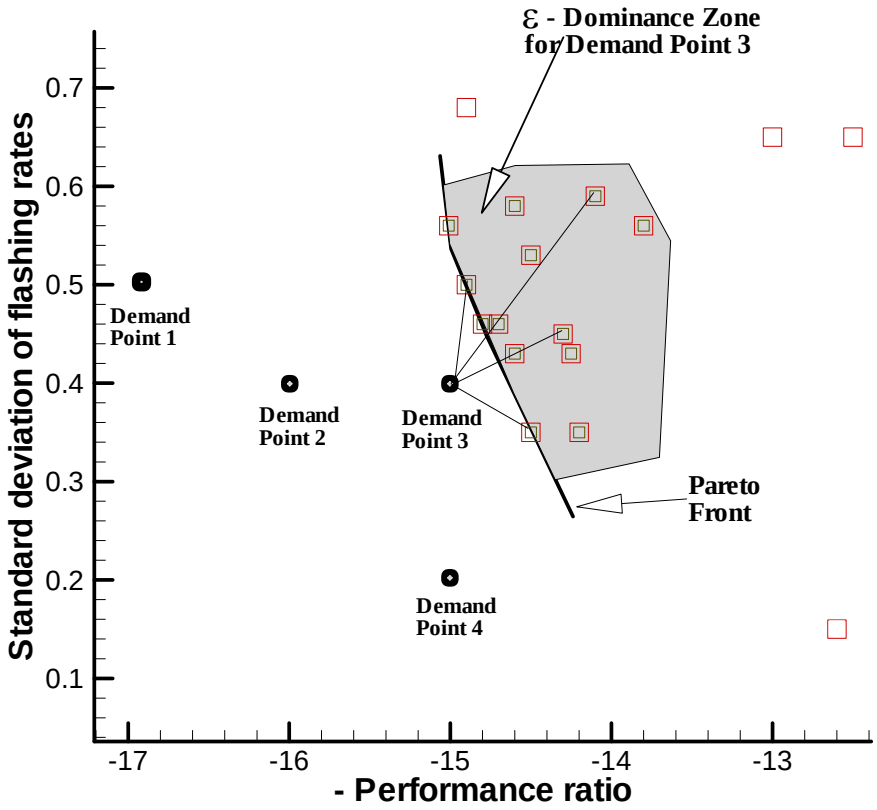

Fig. 4.3 Demand points and the zone of ε-dominance

Table 4.1 The optimum attained for various demand points

S.No.	*Demand point*	*Best optimum obtained*
1	q_1(PR = 17, σ = 0.5)	PR = 15.1, σ = 0.525
2	q_2(PR = 16, σ = 0.4)	PR = 14.9, σ = 0.495
3	q_3(PR = 15, σ = 0.4)	PR = 14.8, σ = 0.452
4	q_4(PR = 15, σ = 0.2)	PR = 14.4, σ = 0.335

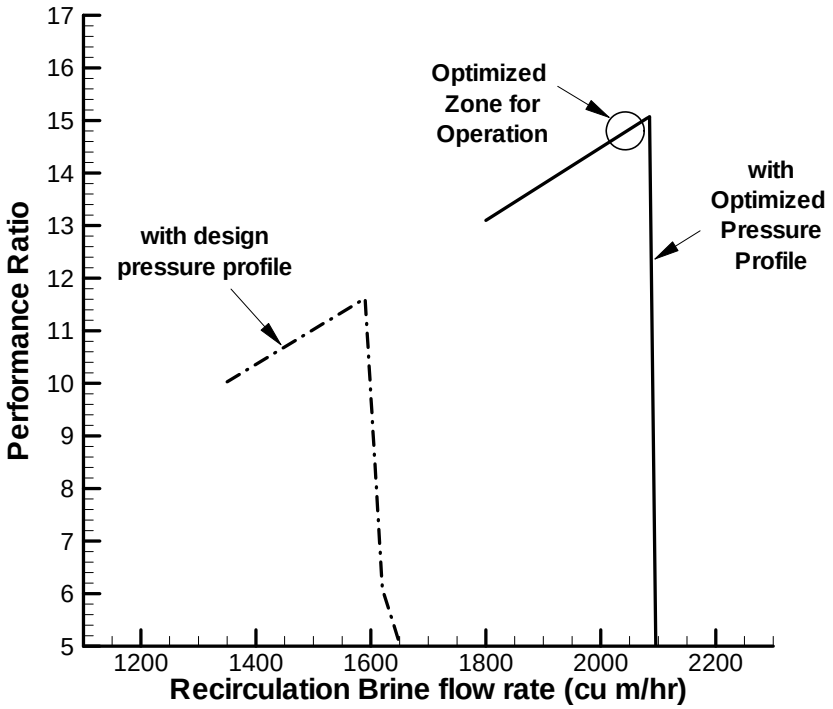

Figure 4.4 PR as a function of RB flow rate, comparison between design and optimized pressure profile (for increased HT area case)

Table 4.2 The details of the optimized steady solution

Description	**Optimized at 120% design HT area**
Capacity	7,526 to 7,599 m^3/day
Top brine temperature	120.10 to 120.11 °C
RB flow rate	2,065 to 2,085 m^3/hr
Brine heater temperature rise	4.4 °C to 4.9 °C
Performance ratio	14.96 to 15.08

Fig. 4.4 shows a sharp drop in PR when the RB flow rate crosses a threshold value (explained earlier). Using the optimized pressure profile an increase in the threshold RB flow rate from 1580 m^3/hr to 2085 m^3/hr was possible. This increase in RB flow rate leads to higher value of PR 15.1.

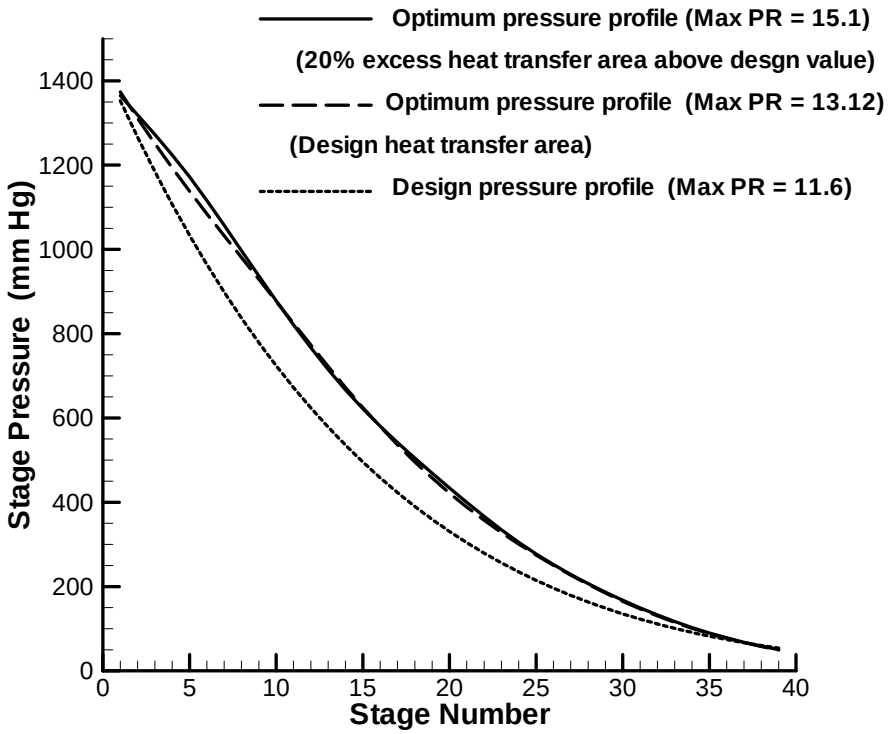

Figure 4.5 The optimized pressure profiles in comparison with design pressure profile

The optimized zone (shown in Fig. 3.16 and 4.4) has to be selected as per the controllability of the process and the instrumentation. This zone has to be sufficiently far from the sharp drop based on final operational considerations. In this report we have studied the maximum theoretically achievable values.

Chapter 5
Startup optimization using GA

A steady state optimum solution for NDDP MSF plant has been obtained in chapter-3. The difficult question that arises is how to attain this optimum with an appropriate startup. This requires a new optimization study to be performed, which regulates the shape of the recirculation flow transient and the pressure transient. Fig. 5.1 shows a schematic of the procedure adopted while coupling MSFSIM with GA for startup optimization. Our objective is to optimize the recirculation transient and pressure transient during startup so that it reaches the stable optimum.

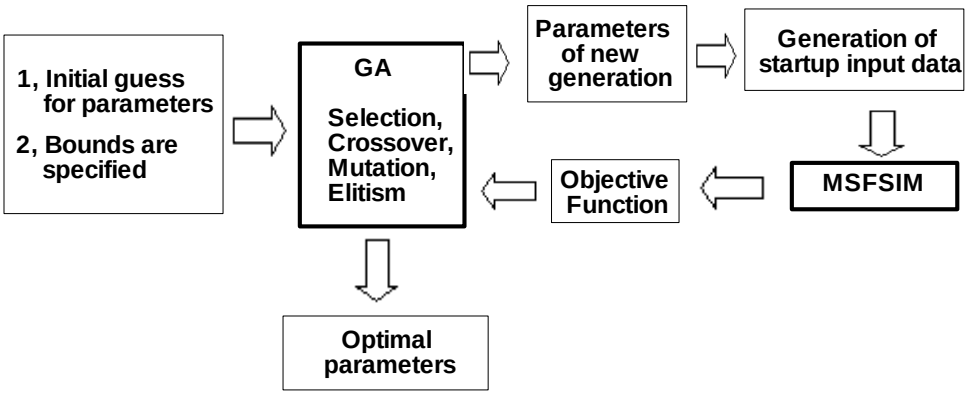

Figure 5.1 The schematic showing the procedure of coupled MSFSIM with GA

The objective function (OF) to be maximized, is chosen such that it reaches the value of PR=15.0 (steady state optimum) in minimum amount of time

$$OF = 300.\left(\frac{e^{-Max\left\{ \left| PR - 15. \right| \;,\; Ptol \right\}}}{N_t} \right)$$

Where PR is the performance ratio and N_t is the time taken for the production to stabilize The objective function chosen enforces penalty for not reaching PR=15.0. This penalty function approach brings about faster convergence [13]. *Ptol* = 0.2, is the tolerance allowed *i.e.* under optimized condition PR should reach to a value within 14.8 to 15.2. The factor of 300 is to make value of *OF* approach unity on convergence. This would make the convergence faster [12].

4.1 Parameterization of the problem

9 control parameters have been chosen in this problem. Of these 6 parameters are used for representing the recirculating brine flow control with respect to startup is shown in Fig. 5.2.

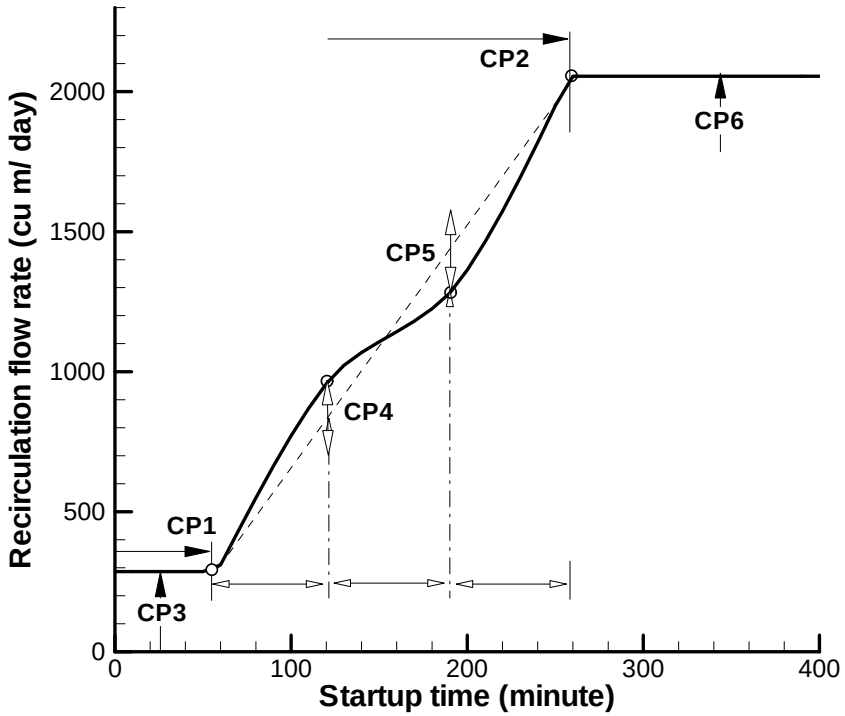

Figure 5.2 Parameterization of the recirculation curve

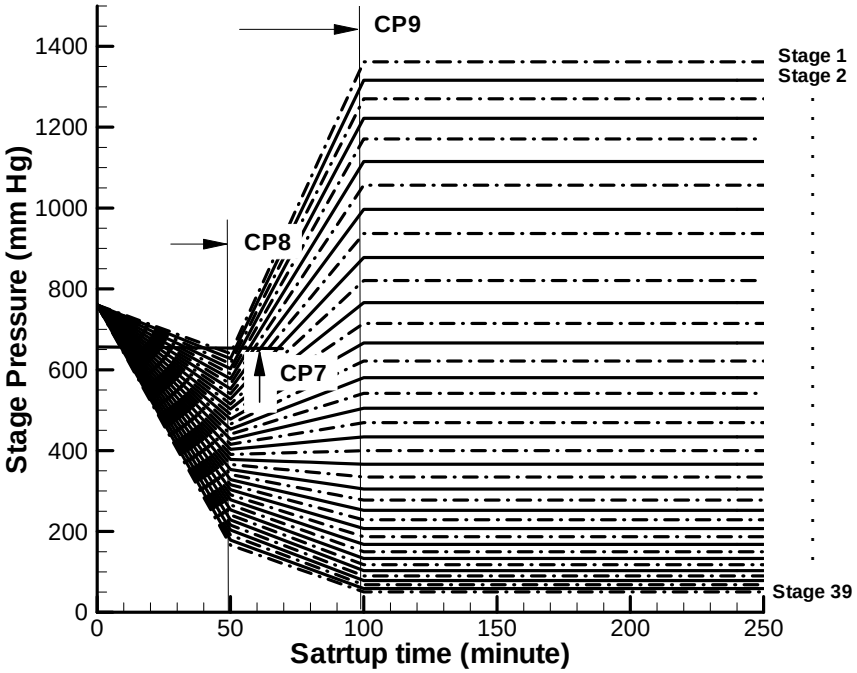

Figure 5.3 Parameterization of the startup pressure profile

3 parameters were used for stage pressure control so that the pressure transient can be controlled as a whole. The pressure transient parameterization is shown in Fig. 5.3. The startup pressure profile saturates to the values of optimized pressure profile

obtained in Section 3. The initial range of optimization for these parameters is given in Table 5.1.

Table 5.1 Parameterization of startup problem

Parameter	Initial Range
Recirculating brine flow rate transient parameters	
CP_1 (time after which RB flow rate increases from its initial value)	30-80 min.
CP_2 (time after which RB flow rate reaches to its final value)	200-500 min
CP_3 (Initial RB flow rate)	200-500 m^3/hr
CP_4(variation over the mean value at time = CP_1+(CP_2- CP_1)/3)	0.6-1.4 times mean value
CP_5(variation over the mean value at time = CP_1+(CP_2- CP_1)*2/3)	0.6-1.4 times mean value
CP_6(final RB flow rate)	2,000 – 2,100 m^3/hr
Pressure profile transient parameters	
CP_7 (Minimum pressure the first stage attains during the startup)	500-700 mm Hg
CP_8 (time at which pressure profile starts recovering from its dip)	60- 200 min.
CP_9 (time at which pressure profile attains its final values)	120-300 min.

4.2 Results of startup optimization (target PR=15.1)

Table 3.2 gives the details fixing the parameters within GA. Fig. 5.5 gives the evolution of the objective function with the generation. The saturation in objective function is attained after 72 generations.

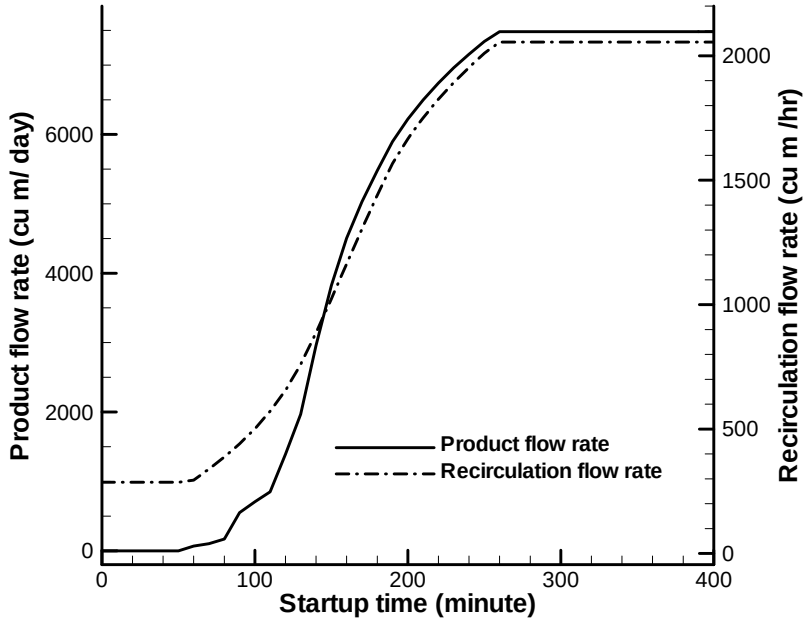

Figure 5.4 The optimized recirculation curve and its corresponding production curve

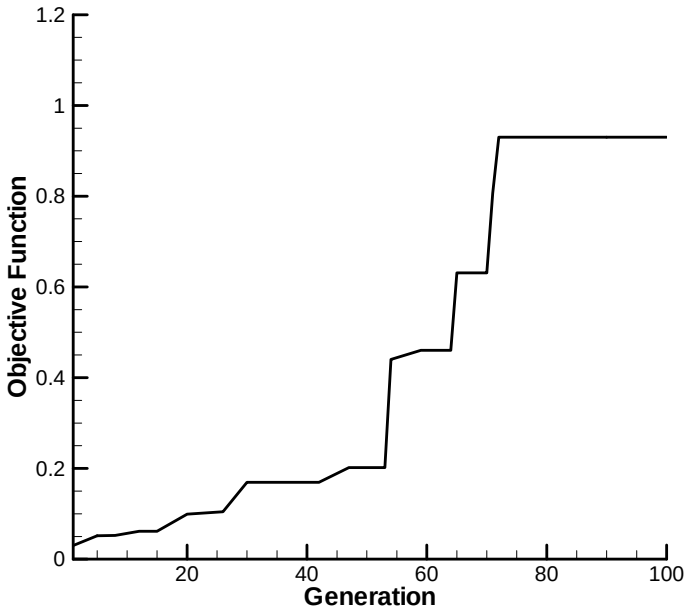

Figure 5.5 Evolution of objective function with generation

The optimized sets of parameters are given in Table 5.2. Fig. 5.4 gives the optimized recirculation flow rate and production rate as function of startup time. Fig 5.6 shows the final optimized pressure transient. Fig 5.7 gives the feed, reject and blow down flow rates during startup under optimum condition. The desired steady state optimum production rate could be reached in minimum amount of 265 minutes (see Fig. 5.4).

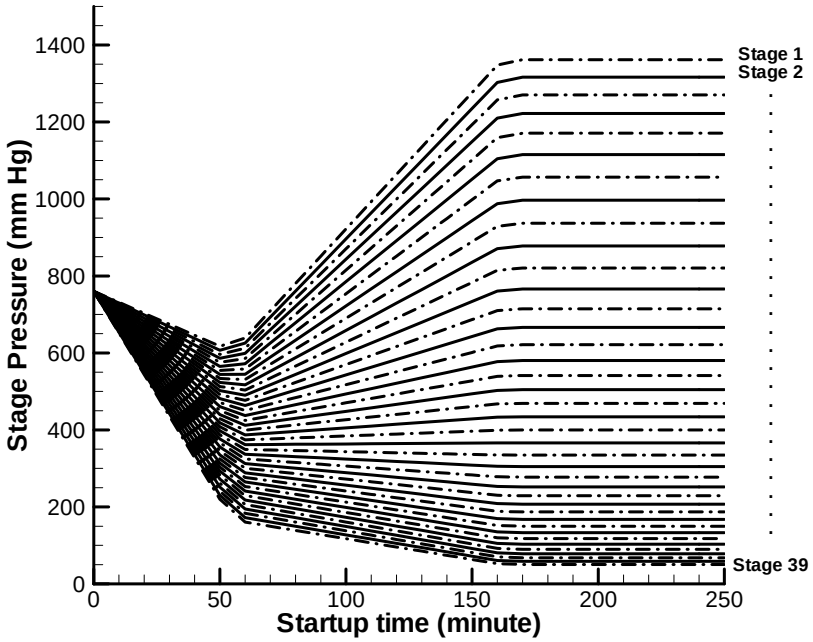

Figure 5.6 The final optimized pressure transient

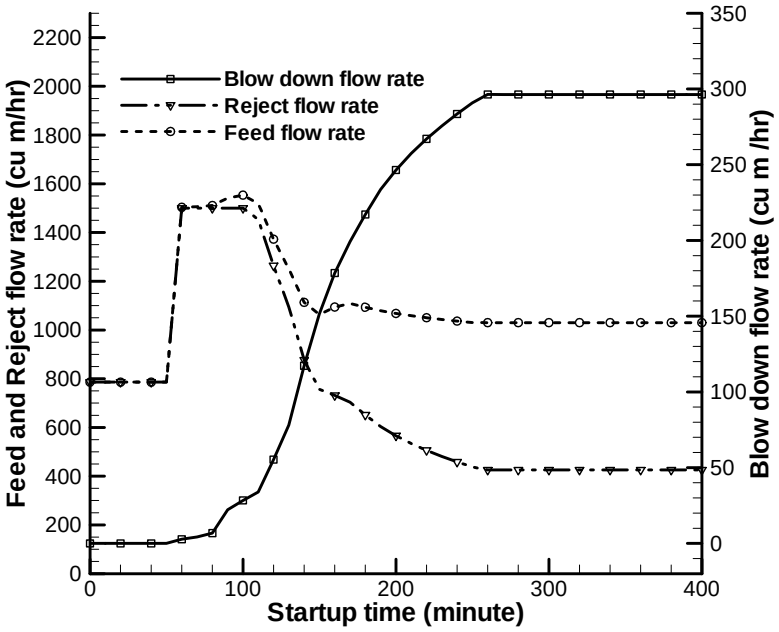

Figure 5.7 The optimized feed, reject and blow down rates during startup

Table 5.2 Details of the optimized parameters

Control Parameter	**Final optimized values**
CP_1	58 min.
CP_2	258 min.
CP_3	286 m^3/hr
CP_4	1.15 times mean value
CP_5	1.1 times mean value
CP_6	2055. m^3/hr
CP_7	603 mm Hg
CP_8	55. min.
CP_9	107 min.
Time to reach the desired production rate	265 minute

Chapter 6
Conclusions and Future scope

A method for process optimization of multi-stage flash desalination process using genetic algorithm has been described in this report. This method can handle multiple objectives as well multiple constraints. This process has enabled us to optimally fix the steady state pressure of the ejectors of the MSF plant to get a maximum performance ratio. Leading to the overall optimization of the process plant. The optimal startup procedure was also an outcome of the "startup optimization" conducted. This would be very useful for the personnel at the plant to guide them to the final optimal steady state.

MSFSIM, a simulator for desalination process was developed and extensively validated with pilot plant data. MSFSIM has been used for the simulation of NDDP-MSF plant which is under construction at Kalpakkam, India. A Graphic user interface is developed to enhance the usability of the code MSFSIM (Appendix-B discusses about the simulator under startup condition). MSFSIM has been coupled with Genetic Algorithms so that process optimization could be studied. The most important parameters in the control of MSF plant are the steady state stage pressures and recirculation flow rate.

It was observed that an improved performance ratio was increasing the variation in flashing rates in the stages- an undesirable feature. An extensive multi objective optimization study was conducted using PR as 1^{st} objective function and variation of stage flashing rates from their mean as 2^{nd} objective function. A substantial increase in the performance ratio from design value of 9.0 to 13.1 (stable optimized value) was obtained. This is 45% improvement over design value.

The plant under construction at Kalpakkam has a 20% excess heat transfer area above the design value (for seasonal requirements). The GA based optimization carried out under changed scenario has yielded a PR of 15.1. This is 68% improvement over design value.

The crucial aspect of MSF-plant operation is its startup. The startup optimization performed gives a quantitative guide lines on how to go about during the startup of the MSF-plant. The startup pressure characteristics and the corresponding recirculation flow rate transient were optimized. The target of the optimization was to reach the production corresponding to PR of 15.1 in minimum amount of time. The optimizer was able to minimize the time of startup to 260 minute.

Further work is being planned on the following aspects:

1. The NDDP-MSF process simulator will be used to generate the Jacobian matrix J so that it can inverse modeling can be done to determine the set points for the control system of the MSF plant. The complete configuration of the MSF plant can be represented by the vector space $\vec{x}$ constituting of variables like recirculation flow rate, steam mass flow rate, etc. Let there be k state variables

$s_i = s_i(\vec{x}),\ i = 1,...,k$ like performance ratio, distillate production rate, etc.; these is the output from the MSF plant. Also there are k target state variables constituting vector $\vec{t}$ (defined by the user) such that $t_i = t_i(\vec{x}),\ i = 1,...,k$. We define the desired change in state variable, $e_i = t_i - s_i,\ i = 1,...,k$. The process control problem to find $t_i = s_i(\vec{x}),\ i = 1,...,k$ (6.1)

Unfortunately, there may not always be a solution to (6.1), and there may not be a unique (best) solution. Even in well-behaved situations, there may be no closed form equation for the solution. We can, however, use iterative methods to approximate a good solution. For this, the functions $s_i(\vec{x}),\ i = 1,...,k$ are linearly approximated using the Jacobian matrix. The Jacobian matrix J is a function of the $\vec{x}$ values and is defined by

$$J(\vec{x}) = \left(\frac{\partial s_i}{\partial x_j} \right)_{i,j} \quad (6.2)$$

J is the Jacobian matrix which can be generated by MSFSIM code. The basic equation for forward dynamics that describes the velocities of the state vectors can be written as follows (using dot notation for first derivatives)

$$\dot{\vec{s}} = J(\vec{x})\ \dot{\vec{x}} \quad (6.3)$$

The Jacobian leads to an iterative method for solving equation (6.1). Suppose we perturb from a current steady state by value of Δs_i and Δx_i. Equation (6.3) can be approximated as

$$\Delta\vec{s} \approx J(\vec{x})\ \Delta\vec{x} \quad (6.4)$$

The idea is that the $\Delta\vec{x}$ value should chosen so that $\Delta\vec{s}$ is approximately equal to $\vec{e}$, so that the system follows the desired target transient distribution.

i.e $\vec{e} \approx J(\vec{x})\ \Delta\vec{x}$ (6.5)

2. Design of an Artificial Neural Network based expert system to predict the plant performance for a given set of operating conditions.

3. Development of multi objective optimization technique based on Ant Colony Optimization where discrete parametric simulation has advantages compared to Genetic Algorithms.

Nomenclature

A_i	Outer surface area of all tubes in the stage i (m^2)
C_B	Specific heat of brine (J / kg K)
C_W	Specific heat of water (J / kg K)
C_T	Specific heat of tube material (J / kg K)
d_i, d_o, $\bar{d}_T$	Inner, outer and log mean diameter of the recirculating tubes (m)
EBP	Elevation in boiling point (K)
E_L	Enthalpy of saturated liquid (J/kg)
E_S	Enthalpy of saturated steam (J/kg)
f_i	Flashing in stage i (m^3/hr)
g	gravitational constant (m/s^2)
h_i, h_o	Heat transfer coefficient inside and outside recirculating tubes (W/m^2 K)
J	Jacobian matrix
k_B, k_W	Thermal conductivity of the brine and recirculating tube (W/m K)
L	Length of the tube (m)
OF	Objective function
n	Number of stages
N_t	Time required for startup (s)
P_i	Pressure in stage i (mm Hg)
S_{BD}	Blow down salinity
t	Time (s)
$T_{B,i}$,$T_{B,i+1}$	Inlet & outlet brine temperature of stage i (K)
T_C	Re-circulating Brine temperature (K)
$T_{Sat,i}$	Saturation temperature for water in stage i (K)
T_W	Tube wall temperature (K)
U_O	Overall heat transfer coefficient (W/m^2 K)
V	Velocity of brine inside the tube (m/s)
$V_{RB,Max}$	Maximum velocity in the recirculating brine (m/s)
W_S	Steam flow rate in brine heater (kg/s)
$W_{O,i}$	Brine holdup in the evaporator stage i (kg)
$W_{P,i}$	Water flow rate in the distillate corridor stage i (kg/s)
W_{Di}	Re-flashing vapor rate from stage i (kg/s)
W_{Fi}	Flashing vapor flow rate from stage i (kg/s)
W_{RSi}	Brine hold up inside tubes in stage i (kg)
$W_{R,i}$,$W_{R,i+1}$	Inlet & outlet brine flow rate of stage i (kg/s)
W_T	Weight of tubes per stage (kg)
$[\ ]^T$	Transpose of a vector

Greek

α, β	Weights of objective functions
κ	Coefficient of heat loss
λ_b	Latent heat of recirculating brine (J/kg)
λ_w	Latent heat of product water (J/kg)
μ_B, μ_W	Viscosity of the brine at brine temperature and at wall temperature (kg/m K)
σ	Average variation of the flashing rate in all the stages (m^3/hr)

Acknowledgements

The Authors would give their sincere thanks to Shri M.Chatterjee, MDD who was a part of the team involved in the MSFSIM development, and to Dr P.K.Tewari, Head Desalination Division for providing the validation data of the pilot plant.

References

1. G.N. Sashi Kumar, M. Chatterjee, A.K. Mahendra, P.K. Tewari, V.D. Puranik and G. Gouthaman, Proceedings of International Conference on Separation Science, 30th July-3rd August 2002, IIT Kharagpur, India.
2. R.K. Verma, Technical aspects of coupling a 6300 m3/day MSF-RO desalination plant to a PHWR, International Atomic Energy Agency, Vienna (Austria), IAEA-TECDOC-1056 , 1998.
3. G.N. Sashi Kumar, M. Chatterjee, A.K. Mahendra, P.K. Tewari, V.D. Puranik and G. Gouthaman, "Advances in Separation Processes", Allied publishers pvt. ltd., 2005, pages: 181-190
4. M. Chatterjee, G.N. Sashi Kumar, A.K. Mahendra, V.D. Puranik, P.K. Tewari and G. Gouthaman, Proceedings of CHEMCON 19th – 22nd December, 2002, Hyderabad, India
5. M. Chatterjee, G.N. Sashi Kumar, A.K. Mahendra, A. Sanyal and G. Gouthaman, NDDP Multi-Stage Flash Desalination process Simulator Design (Part-1), BARC report BARC/2006/E/011, 2006.
6. G.N. Sashi Kumar, A.K. Mahendra, A. Sanyal and G. Gouthaman, "Genetic Algorithm Based Optimization of a Multi-Stage Flash Desalination Plant", Desalination and Water Treatment, Vol. 1, Page 88-106, 2009.
7. M.A. Darwish, M.M. El-Rafaee, M. Abdel-Jawad, Desalination 100, (1995) 35-64.
8. P. Fiorini , E. Sciubba, Desalination 136(2001) 177-188.
9. R.L. Haupt and S.E. Haupt, Practical genetic algorithms, Wiley-Interscience - John wiley & sons, Inc., 2004.
10. A.K. Mahendra, A. Sanyal and G. Gouthaman, GA based Optimization of Process Network, MDD Internal Report, MDD, BARC, May 2003.
11. G.N. Sashi Kumar, A.K. Mahendra and S.M. Deshpande, Optimization of airfoil shape using genetic algorithm and grid free solver, Proceedings of 7th Aeronautical Society of India CFD International Conference, 11th -12th August, 2004, Bangalore, India
12. G.N.Sashi Kumar, Shape Optimization using a Meshless Flow Solver and Modern Optimization Techniques. MSc(Engg.) Thesis, Department of Aerospace Engineering, Indian Institute of science, Bangalore, November 2006.
13. G.N. Sashi Kumar, A.K. Mahendra and S.M. Deshpande, "Optimization using Genetic Algorithm and Grid-Free CFD solver, Intl. society of CFD / CFD Journal, Volume 16, No.4, pp 425-433, 2008.
14. David Schaffer J., "Multiple Objective Optimization with Vector Evaluated Genetic Algorithms.– In: Genetic Algorithms and Their Applications: Proc. of the

First International Conference on Genetic Algorithms, Lawrence Erlbaum, pp 93-100, 1985.
15. David E.Goldberg, "Genetic algorithms in search, optimization and machine learning", Addison -Wesley Publishing Company, Inc., Reading, 1989.
16. Carlos M. Fonseca and Peter J. Fleming, "Genetic Algorithms for Multiobjective Optimization: Formulation, Discussion and Generalization", Genetic Algorithms: Proceedings of the Fifth International Conference (S. Forrest, ed.), San Mateo, CA: Morgan Kaufmann, July 1993.
17. Murata T., H.Ishibuchi nad H. Tanaka, Multi-objective genetic algorithm and its application to flowshop scheduling', Computers and Industrial Engineering, Vol 30, No. 4, pp 957-968, sept 1996.
18. J. Horn, N. Nafpliotis and D.E. Goldberg, 'A niched pareto genetic algorithm for multiobjective optimization', 1st IEEE conference on Evolutionary Computation, IEEE world congress on Computational intelligence, Volume 1, pp 82-87, 1994.
19. Srinivas, N., K. Deb., "Multiobjective Optimization Using Nondominated Sorting in Genetic Algorithms", Evolutionary Computation, Vol. **2**, No. 3, pp 221-248, Fall 1994.
20. K. Deb, "Multi-objective optimization using evolutionary algorithms", John Wiley & sons (Asia) Pte ltd., Singapore, 2001.
21. Cochran j. K., S.M. Horng and Fowler J.W., "A multi-population genetic algorithm to solve multi-objective scheduling problems for parallel machine", Computers and Operations Research, Volume 30 , Issue 7, pp 1087 - 1102 , June 2003 –MPGA
22. Deb K., Sundar J., Bhaskara U., Chaudhuri S.: *Reference Point Based Multi-Objective Optimization Using Evolutionary Algorithms,* ISSN International Journal of ComputationalIntelligence Research, 2, 3 (2006) 273-286.
23. A.K. Mahendra, A. Sanyal, G. Gouthaman, T.K. Bera, Genetic Algorithm based Separation Cascade Optimization, 10th SPLG, 11th -14th August 2008, Angra dos Reis, Brazil
24. G.N. Sashi Kumar, A.K. Mahendra and S.V. Raghurama Rao, AIAA paper No. 2007-3830., 18th AIAA-CFD conference Miami, FL, June 25th –28th , 2007.
25. McCabe, Warren L. and Julian C. Smith, Unit Operations of Chemical Engineering, McGraw-Hill Higher Education, Singapore, 6th Edition, 2001.
26. Fichtner – Handbook by H.E.Homig, Vulkan Verlag, Essen, 1978.

Appendix-A

A.1 Model equations for the MSF plant simulation

Heat balance for tube in brine heater

$$\frac{dT_{w,i}}{dt} = \kappa(\Delta E_{S,BH}) - \Delta\tilde{T} \tag{A1}$$

$$where\ \Delta E_{S,BH} = \frac{W_S(E_S - E_L)}{C_T W_T}\ \ and\ \ \Delta\tilde{T} = \frac{U_{O,i}A_i(T_{W,i} - 0.5(T_{C,i} + T_{B,i}))}{C_T W_T}$$

Heat balance for brine in brine heater

$$\frac{dT_{B,i}}{dt} = \kappa(\Delta\tilde{T}_B) - \Delta\tilde{T}_C \tag{A2}$$

$$where\ \Delta\tilde{T}_B = \frac{U_{o,i}\ A_i\ (T_{W,i} - 0.5(T_{C,i} + T_{B,i}))}{C_B\ W_{RS,i}}\ \ and\ \ \Delta\tilde{T}_C = \frac{W_{R,i}\ (T_{B,i} - T_{C,i})}{W_{RS,i}}$$

Heat balance for Coolant in evaporator

$$\frac{dT_{C,i}}{dt} = \phi\ T_{W,i+1} - (\frac{\phi}{2} - \varphi)\ T_{C,i} + \varphi\ T_{C,i+1} \tag{A3}$$

$$where\quad \phi = \frac{U_{O,i+1}\ A_{i+1}}{C_{B,i}\ W_{RS,i+1}},\ \varphi = \frac{W_{R,i}}{W_{RS,i+1}}$$

Heat balance for Vapor in evaporator

$$\frac{dT_{W,i+1}}{dt} = \eta(E_{S,i} - E_{L,i}) - \gamma\left(T_{W,i+1} - \frac{T_{C,i} + T_{C,i+1}}{2}\right) \tag{A4}$$

$$where\ \ \eta = \frac{\kappa(W_{F,i} + W_{D,i})}{C_T\ W_{T,i+1}},\ \ \gamma = \frac{U_{O,i+1}\ A_{i+1}}{C_T\ W_{T,i+1}}$$

Heat balance for Brine in evaporator

$$\frac{dT_{B,i+1}}{dt} = \frac{W_{R,i}\ T_{B,i} - W_{R,i+1}\ T_{B,i+1}}{W_{O,i}} - \frac{W_{F,i}\ E_{S,i+1}}{C_B\ W_{O,i}} \tag{A5}$$

Where

$$W_{F,i} = \frac{W_{R,i}C_{B,i}(T_{B,i} - T_{Sat,i} - EBP)}{\lambda_B} \tag{A6}$$

$$W_{D,i} = \frac{W_{P,i}C_{W,i}(T_{Sat,i-1} - T_{Sat,i})}{\lambda_W} \tag{A7}$$

$$W_{R,i+1} = W_{R,i} - W_{F,i} \tag{A8}$$

$$W_{P,i+1} = W_{P,i} + W_{F,i} \tag{A9}$$

$$\frac{1}{U_o} = \frac{d_o}{d_i}\frac{1}{h_i} + \frac{(d_o - d_i)/2}{\bar{d}_t}\frac{d_o}{k_w} + \frac{1}{h_o} + FF \tag{A10}$$

FF is the fouling factor which is taken to be between 0.09 to 0.15 m^2K/kW (time dependent) for the evaporators and where as for brine heater this value is taken as 0.25 m^2K/kW. Selection of such high design fouling factors for the MSF plants will allow to

operate these plants at TBT equal to or even higher than maximum design values. This results in higher productivity.

Where vapor side film heat transfer coefficient, h_o [25] is given by (Nusselt equation)

$$h_o = 0.729 \times \left(\frac{k_B^3 . g . \rho_B^2}{d_o . \Delta T . N . \mu_B} \right)^{0.25} (E_S - E_L)^{0.25} \quad \text{(A11)}$$

$$\Delta T = T_{vapor} - 0.75(T_{vapor} - T_{wall}) \quad \text{(A12)}$$

N is the number of horizontal tubes in the stack
And brine side convective heat transfer coefficient, h_i [25] is given by (Sieder-Tate equation)

$$h_i = 0.027 \times \frac{k_B}{d_i} \left(\frac{d_i . V . \rho_B}{\mu_B} \right)^{0.8} \left(\frac{C_B . \mu_B}{k_B} \right)^{0.33} \left(\frac{\mu}{\mu_w} \right)^{0.14} \quad (\text{Re} > 10{,}000) \quad \text{(A13)}$$

For A_i, $T_{B,i}$, $T_{C,i}$, $T_{BW,i}$, $W_{RS,i}$ and $U_{o,i}$ where i=1 corresponds to brine heater and i = 2 to 40 correspond to stages 1 to 39.
For $W_{F,i}$, $W_{D,i}$, $W_{P,i}$ i=1 to 39 corresponds to stages 1 to 39.

A.2 Correlations for physical properties of Brine [26]

1.**Density**
Validity : Salinity (S) = 0 to 160 gm/kg (i.e. 0 - 1,60,000ppm)
Temperature (T) = 10 to 180 ^oC

Density (gm/cm^3) = $0.5\, a_0 + a_1 (Y) + a_2(2Y^2 - 1) + a_3(4Y^3 - 3Y)$ (A14)
where $Y = (2T - 200) / 160$
$a_0 = 2.016110 + 0.115313\, X + 0.000326\, (2X^2 - 1)$
$a_1 = -0.05410 + 0.001571\, X - 0.000423\, (2X^2 - 1)$
$a_2 = -0.006124 + 0.001740\, X - 0.000009\, (2X^2 - 1)$
$a_3 = 0.000346 + 0.000087\, X - 0.000053\, (2X^2 - 1)$
and $X = (2S - 150) / 150$

2.**Viscosity**
Validity : Salinity (S) = 0 to 130 gm/kg (i.e. 0 - 1,30,000ppm)
Temperature (T) = 10 to 150 ^oC

Viscosity (cP) = $N_W * N_R$
Viscosity of pure water, $N_W = \exp\{-3.79418 + 6047.129/(139.18 + T)\}$ (A15)
Relative viscosity (N_R) = $1 + a_1 S + a_2 S^2$
where
$a_1 = 1.474 \times 10^{-3} + 1.5 \times 10^{-5}\, T - 3.927 \times 10^{-8}\, T^2$
$a_2 = 1.0734 \times 10^{-5} - 8.5 \times 10^{-8}\, T + 2.23 \times 10^{-10}\, T^2$

3. **Thermal Conductivity**
Validity : Salinity (S) = 0 to 100 gm/kg (i.e. 0 - 1,00,000ppm)
Temperature (T) = 10 to 150 ^oC

Thermal conductivity (W/m.K) = 10^{-3}* ($a_0 + a_1 T + a_2 T^2$) (A16)
$a_0 = 576.6 – 34.64 X + 7.286 X^2$
$a_1 = (1526 + 466.2 X – 226.8 X^2 + 28.67 X^3) * 10^{-3}$
$a_2 = - (581 + 2055 X – 991.6 X^2 + 146.4 X^3) * 10^{-5}$
and $X = 28.17 S / (1000 - S)$

4. **Specific heat capacity**
Validity : Salinity (S) = 0 to 160 gm/kg (i.e. 0 - 1,60,000ppm)
Temperature (T) = 0 to 180 ^oC

Specific heat (J/kg.K) = $a_0 + a_1 T + a_2 T^2 + a_3 T^3$ (A17)
$a_0 = 4206.8 – 6.6197 S + 1.2288*10^{-2} S^2$
$a_1 = -1.1262 + 5.4178*10^{-2} S – 2.2719 *10^{-4} S^2$
$a_2 = 1.2026*10^{-2} - 5.356*10^{-4} S + 1.8906*10^{-6} S^2$
$a_3 = 6.8774*10^{-7} + 1.517*10^{-6} S – 4.4268*10^{-9} S^2$

Specific Enthalpy (kcal/kg) = $h_o + 2.38846*10^{-4} * (a_0 + a_1 T + a_2 T^2 + a_3 T^3)$ (A18)
where $h_o = 2.3*10^{-3} S – 1.03*10^{-4} S^2$

5. **Boiling point elevation**
Validity : Salinity (S) = 20 to 160 gm/kg (i.e. 0 - 1,60,000ppm)
Temperature (T) = 20 to 180 ^oC

Boiling point elevation (K) = $S (a_0 + a_1 S)$ (A19)
$a_0 = (6.71 + 6.43*10^{-2} T + 9.74*10^{-5} T^2) *10^{-3}$
$a_1 = (22.38 + 9.59*10^{-3} T + 9.42*10^{-5} T^2) *10^{-5}$

6. **Vapor pressure**
Validity : Salinity (S) = 0 to 160 gm/kg (i.e. 0 - 1,60,000ppm)
Vapor pressure (bar) = $P_w (1 – 0.000537 S)$ (A20)
where P_w is the vapor pressure of pure water at a given temperature.

Appendix – B

MSFSIM – Startup Calculation

The computer code MSFSIM can be used to simulate the startup characteristics of a MSF desalination process. This is particularly useful for studying the off-design performance of the plant due to sudden change in any operating parameters. Furthermore, start-up and shut down transients require very careful considerations, because of their importance in overall performance of the plant. Process flow diagram for the MSF desalination plant shows several stages for brine flashing, two sections of heat recovery and rejection, a brine heater, a cooling water stream, brine recycle stream, their temperatures, flow rates, salinity and many other parameters. Hence due to the large number of plant operating parameters, modeling of dynamic behavior of the plant is a highly labour intensive task. A simulation tool (like MSFSIM) can only conveniently execute this task for a quick and reliable calculation of the relevant process parameters in order to design the instrumentation and control system.

The validation of the transient version of MSFSIM is discussed in chapter 2. Here the description of the GUI of the transient version of MSFSIM is given. It consists of a fortran code running in the background which solves the ODE's mentioned in Appendix A. There are a few assumptions in coding the MSF system. They include

- The introduction of steam to brine heater is the time=0, pressure is atmospheric.
- The extraction curve of the ejector is known (can be specified by the user).
- The oscillations in the stage brine level are negligible.
- Pressure inside a stage in which flash does not occur is equal to that of the extraction curve of ejector.
- Delay of the valve operation is neglected.

The front end i.e. GUI is made in Visual Basic. The forms used in startup simulation of the MSF desalination plant are almost same as those used for steady state simulation [5]. The main form and the input form (shown in Fig. B.1 and B.2 respectively) are exactly the same as used in steady state simulation. On clicking the "Simulate" button in the main form the " Input Data" form shown in Fig. B.2 opens. In this form the user has to enter five input data for simulation. These are brine recirculation flow rate in m^3/hr, sea water inlet temperature in °C, steam inlet flow rate in kg/minute, steam pressure in bar and brine concentration ratio. These values can be supplied with the help of the adjacent scrollbars. Once the input data is given clicking, when the user press "start-up MSFSIM" button one extra form as shown in Fig. B.3 gets activated. This form fixes the re-circulation pattern and asks two more inputs from the user required for start-up simulation. These are the initial brine recirculation flow rate in m^3/hr at time t=0 minute.

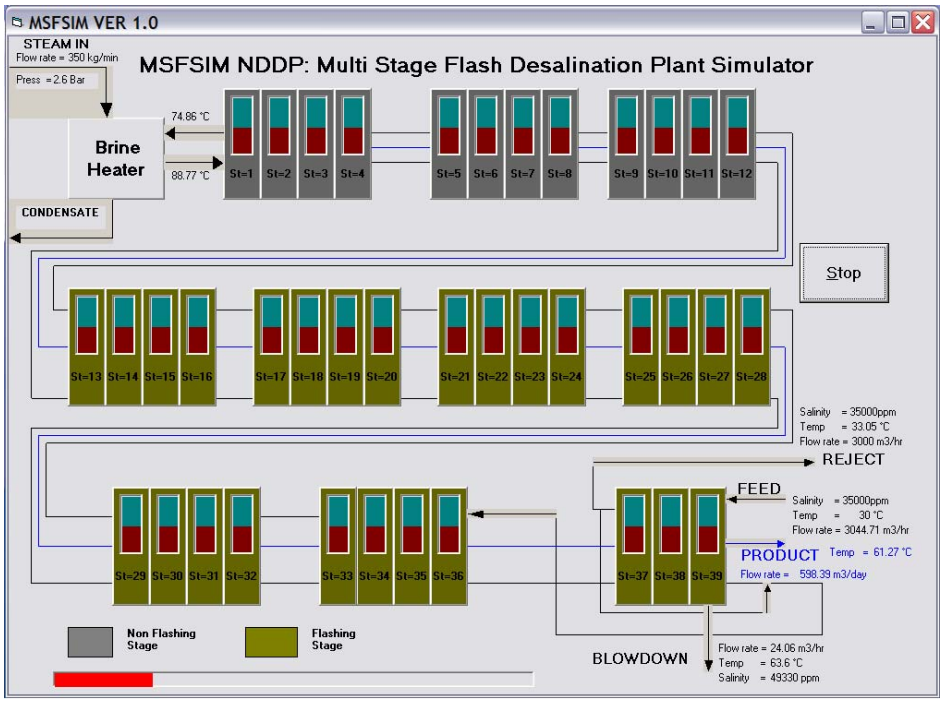

Figure B.1 Opening form of MSFSIM

The user is required to press the button "start simulation" on form B.3 to start the running of the ForTran code at the background. As the code executes, we can observe the progress in the process diagram of the main form.

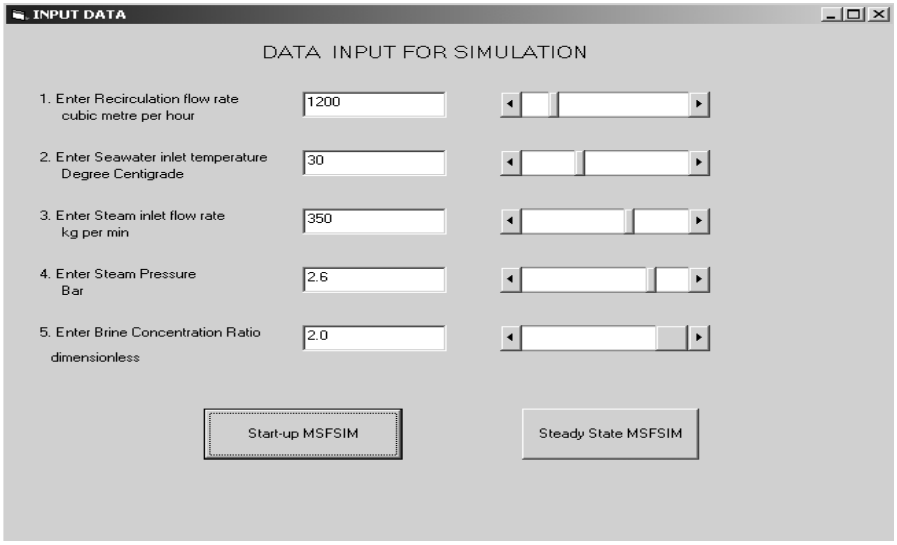

Figure B.2 Data input form

The main form displays flow rate, pressure, temperature, salinity etc. of different streams like heating steam, sea water feed, reject, blow down and product. The display is dynamically updated while the simulation run is carried out. Color of a stage changes

automatically once its starts flashing. If the user clicks on any non flashing stage a child form as shown in Fig. B.4 pops up giving the details of that particular stage. At the top of the form the stage index is depicted.

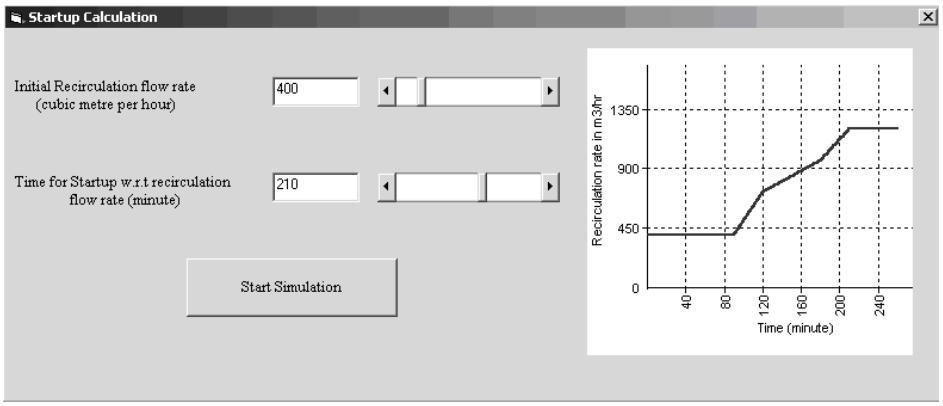

Figure B.3 Additional input required for startup simulation

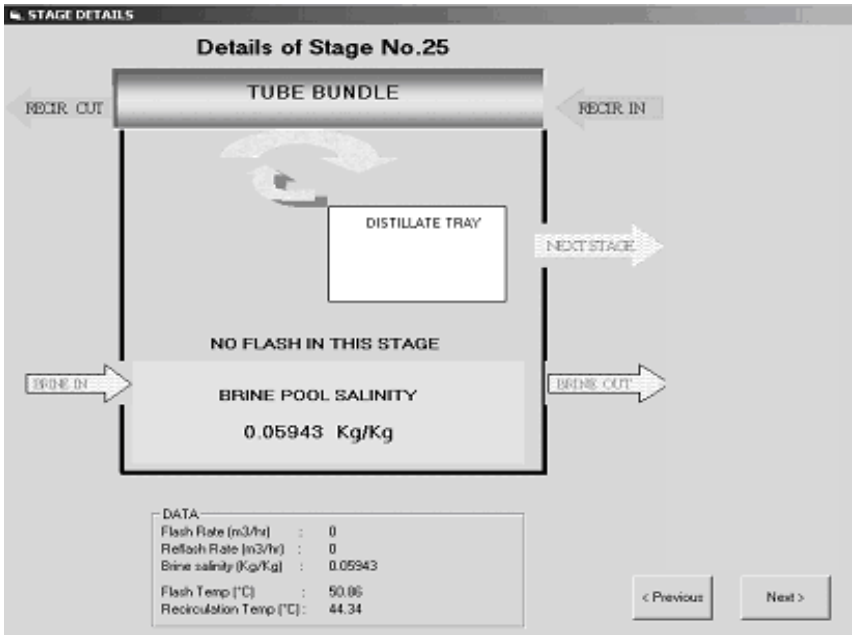

Figure B.4 Details of a non-flashing stage

A message showing “No flash in this stage” indicates presently there is no flashing in this stage. This can also be seen that the distillate tray is completely empty. The values of brine flashing rate from brine pool, brine re-flashing rate from distillate tray, brine salinity, flashing brine temperature and re-circulating brine temperature are summarized at the bottom of the form. One can also see the details of the previous and next stage by clicking the corresponding button at the right bottom corner of the form.

Now, if the user clicks a flashing brine stage the form shown in Fig. B.4 pops up. Here in addition to the information shown as a cloud indicates the brine flashing and its corresponding brine-flashing rate is also shown.

The first result form appears shown in Fig. B.5 consists of 4 plots. Plot 1 in this form shows variation of pressure in 39 stages with time. Plot 2 and 3 shows the variation of brine recirculation flow rate and distillate production rate with time. Plot 4 shows the variation of blow down, reject and feed flow rate with time. To stop the code the user need to press stop simulation button in this simulation result form. The user can also watch the main form to observe the dynamic changes in different parameters like brine heater inlet and outlet temperatures, flow rate, temperature and salinity of reject, blow down and feed etc. during the start-up.

Once the progress bar in the main form stops, indicating end of the program, the second result form shown in Fig. B.6 becomes visible. It consists of 4 plots. Plot 5 in this form shows variation brine heater inlet and outlet temperatures with time. Plot 6 shows stage wise brine flashing rate. Plot 7 shows stage wise flashing brine and re-circulating brine temperatures. Plot 8 shows the stage wise brine salinity attained after start up.

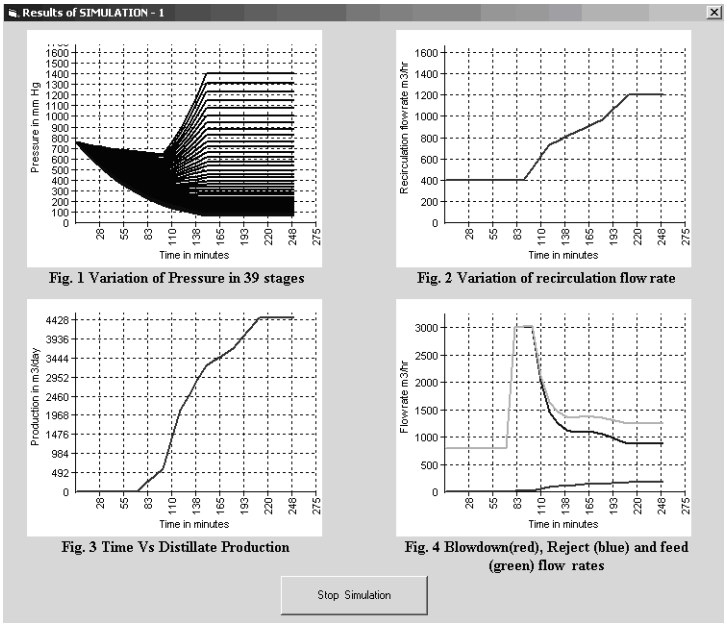

Figure B.5 First result form of start-up simulation

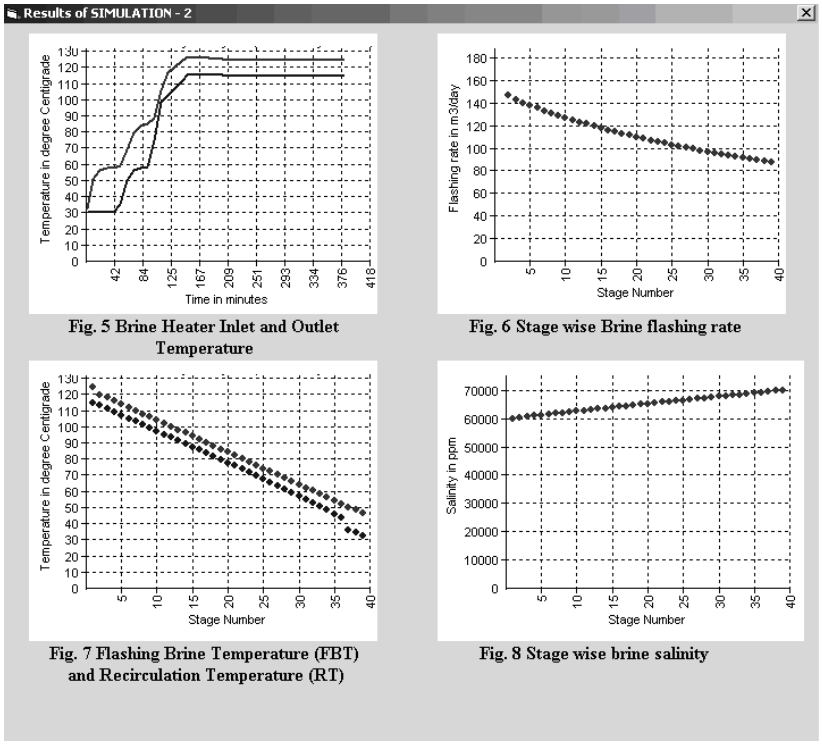

Figure B.6 Second result form of start-up simulation